ELSEVIER

Journal of Organometallic Chemistry 643–644 (2002) 136–153

Journal of Organometallic Chemistry

www.elsevier.com/locate/jorganchem

Enantioselective synthesis of a conformationally rigid, sterically encumbered, 2-arsino-7-phosphanorbornene

Paul A. Gugger [a], Anthony C. Willis [a], S. Bruce Wild [a,*], Graham A. Heath [a], Richard D. Webster [a], John H. Nelson [b,*]

[a] *Research School of Chemistry, Institute of Advanced Studies, Australian National University, Canberra, ACT 0200, Australia*
[b] *Department of Chemistry, University of Nevada, Reno, NV89557-0020, USA*

Received 21 June 2001; accepted 31 August 2001

Dedicated to Professor François Mathey on the occasion of his 60th birthday

Abstract

Convenient access to the enantiomerically pure, conformationally rigid, ligand [5-(dicyclohexylarsino)-2,3-dimethyl-7-phenyl-7-phosphabicyclo[2.2.1]hept-2-ene has been established by intramolecular [4 + 2]-Diels–Alder cycloaddition between dicyclohexylvinylarsine and 3,4-dimethyl-1-phenylphosphole using chiral organopalladium(II) complexes containing orthometallated (*S*)-1-α-(dimethylamino)ethylnaphthalene or (*R*)-2-α-(dimethylamino)ethylnaphthalene as the reaction templates. The ligand was displaced from the palladium complex with cyanide and reacted with $[(\eta^6\text{-arene})RuCl_2]_2$ and NH_4PF_6 to form diastereomeric $[(\eta^6\text{-arene})Ru(P–As)Cl]PF_6$ complexes, chiral at ruthenium. New complexes have been characterized by elemental analyses, electrochemistry, and electronic, circular dichroism, ^1H-, $^1H\{^{31}P\}$-, $^{13}C\{^1H\}$- and $^{31}P\{^1H\}$-NMR spectroscopies, and in several cases, by X-ray crystallography. © 2002 Published by Elsevier Science B.V.

Keywords: Phosphole; Vinylarsine; [4 + 2]-Diels–Alder cycloaddition; Palladium; Ruthenium, X-ray crystallography

1. Introduction

Through studies of the coordination modes of phospholes [1–8], it was discovered that coordination of a phosphole to a transition metal greatly increased the dienic reactivity of the phosphole compared with that of the free ligand [9–13]. This is because coordination to a transition metal reduces the modest degree of cyclic delocalization in the free phosphole [14]. Similar effects accrue by placing strongly electron withdrawing substituents on the phosphole phosphorus atom [13]. Simultaneous coordination of a phosphole and a dieneophilic ligand to a transition metal, in mutually *cis* positions, activates both ligands and promotes facile intramolecular [4 + 2]-Diels–Alder cycloadditions between the two coordinated ligands [15]. Recently, organopalladium complexes containing enantiomerically pure forms of orthopalladated 1-α-(dimethylamino)ethylnaphthalene [16] and 2-α-(dimethylamino)ethylnaphthalene [17] have been used as chiral templates for the asymmetric modification of Diels–Alder cycloadditions with several dieneophilic ligands. Diels–Alder cycloaddition is very sensitive to steric effects, with sterically bulky substituents on either the diene or dieneophile generally suppressing the reaction [18].

Ruthenium(II) complexes of the type $(\pm)$-$[(\eta^6\text{-arene})Ru(AB)X]^+X^-$, where AB is an enantiomerically pure bidentate ligand and X is a halide, are efficient catalysts for the asymmetric transfer hydrogenation of ketones [19], alkenes [20], and imines [21]. The catalytic activity of a ruthenium complex often increases with increased steric bulk of associated ligands [22]. Complexes of the type $(\pm)$-$\{(\eta^6\text{-arene})Ru(AB)\ X]^+X^-$ can be prepared with high diastereoselectivity by intramolecular [4 + 2] Diels–Alder cycloadditions between coordinated 3,4-dimethyl-1-phenylphosphole

* Corresponding authors. Tel.: +61-2-61254236; fax: +61-2-61250750 (SBW). Tel.: +1-775-7846588; fax: +1-775-7846804 (JHN).

E-mail addresses: sbw@rsc.anu.edu.au (S.B. Wild), jhnelson@equinox.unr.edu (J.H. Nelson).

0022-328X/02/$ - see front matter © 2002 Published by Elsevier Science B.V.
PII: S0022-328X(01)01209-8

(DMPP) and a variety of dieneophilic ligands [15k]. The diastereoselectivity of these reactions increases with increasing interligand steric interactions. Within these complexes, ruthenium is a configurationally stable stereocenter. There is considerable current interest in the influence of ligands on the configurational stability of ruthenium stereocenters [23].

Herein, we describe the enantioselective synthesis of an optically pure, conformationally rigid, sterically encumbered 2-arsino-7-phosphanorbornene and two chiral ruthenium derivatives.

2. Experimental

2.1. Reagents and physical measurements

All chemicals were reagent grade and were used as received from commercial sources or synthesized as described below. DMPP [24], the chiral palladium chloride bridged dimers [17,25], and the $[(\eta^6\text{-arene})RuCl_2]_2$ complexes [26] were synthesized by literature methods. Solvents were dried by standard procedures. All reactions involving DMPP were conducted under a purified nitrogen atmosphere by standard Schlenk techniques. Elemental analyses were performed by staff within the Research School of Chemistry. Melting points were determined on a Reichert hot-stage apparatus and are uncorrected. NMR spectra were recorded on $CDCl_3$ solutions with a Varian Inova-500 FT spectrometer operating at 500 MHz for ^1H, 202 MHz for ^{31}P, and 125 MHz for ^{13}C nuclei. Proton and carbon chemical shifts were referenced to residual $CHCl_3$ and phosphorus chemical shifts were referenced to an external 85% aqueous solution of H_3PO_4. All shifts to low field, high frequency, are positive. Electrochemical measurements were recorded using a PAR model 170 or 273A system, controlled by a Macintosh LC 630 computer and MacLab 4e interface running MACLAB E CHEM software (AD Instruments). Scan rates were typically 100 mV s^{-1} for cyclic voltammetry (CV). Electrochemical solutions contained 0.5 mol dm^{-3} $[NBu^n_4][PF_6]$ and ca. 10^{-3} mol dm^{-3} complex in CH_2Cl_2. The solutions were purged and maintained under an atmosphere of N_2. The jacketed cryostatic cell (10 cm^3) contained a platinum disc (1.0 mm diameter) working electrode, platinum wire auxiliary electrode, and Ag–AgCl reference electrode (containing 0.45 M $[Bu^n_4N][PF_6]$ and 0.05 M $[Bu^n_4N][Cl]$) (against which the ferrocene/ferrocenium couple is found at 0.55 V). Measurements were recorded at low temperature using a Lauda model RL6 cryostat bath to circulate dry CH_3OH through the cell jacket. In situ UV–vis–NIR spectra were measured on a Varian Cary SE spectrophotometer at -40 °C by use of an optically transparent thin layer electrochemical (OTTLE) cell placed in the spectrophotometer, as described previously [27]. Optical rotations were measured on a Perkin–Elmer model 241 polarimeter under the specified conditions.

Solutions of $\mathbf{9b}^+$ for EPR and circular dichroism (CD) experiments were prepared by one-electron electrochemical oxidation of **9b** in a divided controlled potential electrolysis cell separated with a porosity no. 5 (1.0–1.7 μm) sintered glass frit. The working and auxiliary electrodes were identically sized Pt mesh plates symmetrically arranged with respect to each other with an Ag wire reference electrode (isolated by a salt bridge) positioned to within 5 mm of the surface of the working electrode. The electrolysis cell was jacketed in a glass sleeve and cooled to 233 K using the Lauda cryostat methanol circulating bath. The volumes of both the working and auxiliary electrode compartments were ca. 25 mL each and were continually purged with argon during the electrolysis. The number of electrons transferred during the bulk oxidation process was calculated from

$$N = Q/nF \quad (1)$$

where N is number of moles of starting compound, Q is the charge (coulombs), n is number of electrons and F is the Faraday constant (96 485 C mol^{-1}). In order to ensure that oxygen was not introduced and to minimize temperature fluctuations during the transfer process, the bottom of the working electrode compartment was connected via glass tubing to an evacuated 2 mm diameter cylindrical quartz EPR tube suspended in a dry ice–EtOH bath maintained at 203 K. Opening the tap on the bottom of the electrolysis cell at the completion of the electrolysis allowed the solution to flow rapidly into the EPR tube which was sealed with a Young's tap before being further cooled in liquid nitrogen. The EPR cell was then transferred to a Bruker ESP 300e spectrometer employing a rectangular TE_{102} cavity with the modulation frequency set at 100 kHz. A similar procedure was used to obtain a solution of $\mathbf{9b}^+$ for the CD experiments using a Jobin Yvon CD6 spectropolarimeter and ensuring the temperature of the solution was at all times ≤ -40 °C.

2.2. Synthesis

2.2.1. Dicyclohexylvinylarsine (Cy_2AsVy) (1)

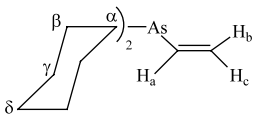

To a solution containing 38.0 g (0.137 mol) Cy_2AsCl [28] in 400 mL of dry diethyl ether was slowly added 100 mL of 1.6 M (0.16 mol) $CH_2CHMgBr$ (Aldrich) at ambient temperature. The reaction mixture was stirred

vigorously for 2 h at ambient temperature and then heated under reflux for 5 h. After cooling to ambient temperature, the mixture was filtered through Celite, concentrated to half volume under vacuum, and washed with 50 mL of saturated aqueous NH_4Cl. The ether layer was separated, dried over anhydrous Na_2SO_4, filtered, and the ether was removed from the filtrate under vacuum. The residue was distilled to obtain the product as a colorless viscous oil; b.p. 122–128 °C (1.5–2.5 mmHg) 11.05 g (30%). Anal. Calc. for $C_{14}H_{25}As$: C, 62.73; H, 9.33. Found: C, 62.56; H, 9.19%. ^{1}H-NMR: δ 6.47 (dd, $^3J(H_aH_b) = 18.6$ Hz, $^3J(H_aH_c) = 11.4$ Hz, 1H, H_a), 5.95 (dd, $^3J(H_aH_c) = 11.4$ Hz. $^2J(H_bH_c) = 2.4$ Hz, 1H, H_c), 5.68 (dd, $^3J(H_aH_b) = 18.6$ Hz, $^2J(H_bH_c) = 2.4$ Hz, 1H, H_b), 1.73 (m, 12H, Cy), 1.25 (m, 10H, Cy). ^{13}C{^{1}H} δ 137.68 (C'_α), 130.34 (C'_β), 34.21 (C_α), 31.63, 30.81 (C_β), 29.95, 27.61 (C_γ), 26.54 (C_δ).

2.2.2. (S)-(+)-[(TMBA)PdCl(DMPP)] (2)

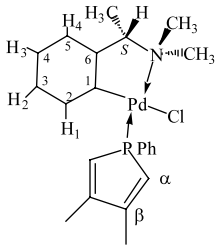

To a solution containing 10.0 g (0.017 mol) [(*S*)-(TMBA)PdCl]$_2$ [25b] in 250 mL of CH_2Cl_2 was added 6.6 g (0.035 mol) DMPP [24]. The resulting deep yellow solution was stirred at ambient temperature for 1 h, the solution volume reduced to 25 mL on a rotary evaporator, and *n*-hexane added. The almost colorless crystals that separated were isolated by filtration, washed with *n*-hexane and diethyl ether and vacuum dried. Yield 15.2 g (92.1%) m.p. 144–146 °C. $[\alpha]_D + 87.0°$ (*c*, 0.2, CH_2Cl_2). CD (molecular ellipticity $[\theta]_\lambda$ (deg cm^2 d mol^{-1}) for $c = 1.04 \times 10^{-4}$ M in CH_2Cl_2 at 25 °C) $[\theta]_{431} = +5686$, $[\theta]_{341} = +6446$, $[\theta]_{317} = -416$, $[\theta]_{299} = +2415$, $[\theta]_{288} = 0$, $[\theta]_{278} = -13\,579$, $[\theta]_{263} = 0$, $[\theta]_{240} = +22\,494$. Anal. Calc. for $C_{22}H_{27}ClNPPd$: C, 55.27; H, 5.65; Cl, 7.42. Found: C, 55.11; H, 5.80; Cl, 7.26%. ^{1}H-NMR: δ 7.88 (m, 2H, H_o), 7.38 (m, 1H, H_p), 7.33 (m, 2H, H_m), 6.99 (dd, $^3J(H_3H_4) = 7.5$ Hz, $^4J(H_2H_4) = 1.0$ Hz, 1H, H_4), 6.96 (apparent td, $^3J(H_2H_3) = {}^3J(H_3H_4) = 7.5$ Hz, $^4J(H_1H_3) = 1.0$ Hz, 1H, H_3), 6.91 (apparent td, $^3J(H_1H_2) = {}^3J(H_2H_3) = 7.5$ Hz, $^4J(H_2H_4) = 1.0$ Hz, 1H, H_2), 6.80 (apparent td, $^3J(H_1H_2) = {}^4J(PH) = 7.5$ Hz, $^4J(H_1H_3) = 1.0$ Hz, 1H, H_1), 6.74 (apparent d quin, $^2J(PH) = 32.0$ Hz, $^4J(HH) = {}^4J(HH) = 1.5$ Hz, 1H, H_α), 6.60 (apparent d quin, $^2J(PH) = 32.5$ Hz, $^4J(HH) = {}^4J(HH) = 1.5$ Hz, 1H, H_α), 3.82 (dq, $^3J(HH) = 6.5$ Hz, $^4J(PH) = 4.5$ Hz, 1H, CH), 2.83 (d, $^4J(PH) = 2.0$ Hz, 3H, NCH_3), 2.69 (d, $^4J(PH) = 2.0$ Hz, 3H, NCH_3), 2.06 (apparent t, $^4J(PH) = {}^4J(HH) = 1.5$ Hz, 3H, DMPP–CH_3), 2.05 (apparent t, $^4J(PH) = {}^4J(HH) = 1.5$ Hz, 3H, DMPP–CH_3), 1.58 (d, $^3J(HH) = 6.5$ Hz, 3H, CCH_3). ^{13}C{^{1}H}-NMR: δ 154.47 (d, $^3J(PC) = 1.9$ Hz, C_6), 152.32 (d, $^2J(PC) = 10.9$ Hz, C_β), 151.17 (d, $^2J(PC) = 10.6$ Hz, C_β), 148.28 (d, $^2J(PC) = 2.8$ Hz, C_1), 136.73 (d, $^3J(PC) = 12.6$ Hz, C_2), 133.66 (d, $^2J(PC) = 13.2$ Hz, C_o), 130.73 (d, $^4J(PC) = 2.5$ Hz, C_β), 128.47 (d, $^3J(PC) = 10.9$ Hz, C_m), 126.61 (d, $^1J(PC) = 52.4$ Hz, C_α), 126.23 (d, $^1J(PC) = 46.3$ Hz, C_i), 125.50 (d, $^1J(PC) = 51.6$ Hz, C_α), 125.43 (d, $^3J(PC) = 5.9$ Hz, C_5), 124.08 (s, C_3), 123.02 (s, C_4), 74.33 (d, $^3J(PC) = 3.0$ Hz, CH), 49.70 (d, $^3J(PC) = 2.6$ Hz, N CH_3), 45.17 (d, $^3J(PC) = 2.1$ Hz, N CH_3), 20.03 (s, CCH_3), 17.52 (d, $^3J(PC) = 12.8$ Hz, DMPP–CH_3). ^{31}P{^{1}H}-NMR: δ 37.8.

2.2.3. (S)-(+)-[(1TMNA)PdCl(DMPP)] (3)

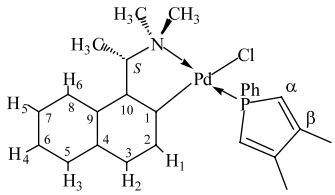

To a suspension of 5.0 g (5.8 mmol) [(*S*)-(1TMNA)PdCl]$_2$ [25a] in 50 mL CH_2Cl_2 was added 2.8 g (14.7 mmol) DMPP. The clear yellow solution was stirred at ambient temperature for 2 h, filtered through Celite, and the solvent removed from the filtrate by rotary evaporation. The resulting foamy solid was washed with *n*-hexane and diethyl ether and vacuum dried to yield 7.34 g (94.5%) of pale yellow microcrystals m.p. 128–130 °C $[\alpha]_D + 334.9°$ (*c*, 0.2, CH_2Cl_2). CD (molecular ellipticity $[\theta]_\lambda$ (deg cm^2 d mol^{-1}) for $c = 1 \times 10^{-4}$ M in CH_2Cl_2 at 25 °C) $[\theta]_{332} = +928$, $[\theta]_{290} = +5572$, $[\theta]_{258} = +6704$, $[\theta]_{250} = 0$, $[\theta]_{247} = -1138$, $[\theta]_{243} = 0$. Anal. Calc. for $C_{26}H_{29}ClNPPd$: C, 59.13; H, 5.49; Cl, 6.71. Found: C, 58.92; H, 5.62; Cl, 6.57%. ^{1}H-NMR: δ 7.94 (m, 2H, H_o), 7.71 (dd, $^3J(H_3H_4) = 8.5$ Hz, $^4J(H_3H_5) = 1.5$ Hz, 1H, H_3), 7.69 (d, $^3J(H_5H_6) = 8.0$ Hz, 1H, H_6), 7.39 (m, 4H, 2H_m, H_p, H_4), 7.34 (ddd, $^3J(H_5H_6) = 8.0$ Hz, $^3J(H_4H_5) = 7.0$ Hz, $^4J(H_3H_5) = 1.5$ Hz, 1H, H_5), 7.31 (d, $^3J(H_1H_2) = 8.0$ Hz, 1H, H_2) 7.14 (dd, $^3J(H_1H_2) = 8.0$ Hz, $^4J(PH) = 5.8$ Hz, 1H, H_1), 6.94 (apparent d quin, $^2J(PH) = 32$. Hz, $^4J(H_\alpha H_{\alpha'}) = {}^4J(HH) = 1.5$ Hz, 1H, H_α), 6.46 (apparent d quin, $^2J(PH) = 32$ Hz, $^4J(H_\alpha H_{\alpha'}) = {}^4J$ (HH) = 1.5 Hz, 1H, $H_{\alpha'}$), 4.32 (apparent quin, $^3J(HH) = {}^4J(PH) = 6.5$ Hz, 1H, CH), 2.91 (d, $^4J(PH) = 3.0$ Hz, 3H, N CH_3), 2.76 (d, $^4J(PH) = 1.0$ Hz, 3H, N CH_3), 2.08 (apparent t, $^4J(HH) = {}^4J(PH) = 1.5$ Hz, 3H, DMPP–CH_3), 2.04

(apparent t, $^4J(HH) = {}^4J(PH) = 1.5$ Hz, 3H, DMPP–CH_3), 1.86 (d, $^3J(HH) = 6.5$ Hz, 3H, CCH_3). $^{13}C\{^1H\}$-NMR: δ 153.77 (d, $^2J(PC) = 11.2$ Hz, C_β), 150.17 (d, $^2J(PC) = 10.2$ Hz, C_β), 149.61 (d, $^2J(PC) = 1.6$ Hz, C_1), 147.04 (d, $^3J(PC) = 2.1$ Hz, C_{10}), 135.21 (d, $^3J(PC) = 13.0$ Hz, C_2), 133.75 (d, $^2J(PC) = 13.1$ Hz, C_o), 131.05 (s, C_9), 130.86 (d, $^4J(PC) = 2.4$ Hz, C_p), 129.04 (s, C_4), 128.62 (d, $^3J(PC) = 11.1$ Hz, C_m), 127.67 (d, $^1J(PC) = 52.9$ Hz, C_α), 126.34 (d, $^1J(PC) = 46.0$ Hz, C_i), 125.79 (s, C_7), 124.99 (d, $^4J(PC) = 5.8$ Hz, C_3), 124.35 (d, $^1J(PC) = 50.4$ Hz, $C_{\alpha'}$), 124.11 (s, C_6), 123.06 (s, C_8), 72.67 (d, $^3J(PC) = 2.9$ Hz, CH), 51.03 (d, $^3J(PC) = 2.6$ Hz, N CH_3), 47.59 (d, $^3J(PC) = 1.8$ Hz, N CH_3), 23.33 (s, C CH_3), 17.64 (d, $^3J(PC) = 9.7$ Hz, DMPP–CH_3), 17.54 (d, $^3J(PC) = 10.1$ Hz, DMPP–CH_3). $^{31}P\{^1H\}$-NMR: δ 37.3.

2.2.4. (R)-(−)-[(2TMNA)PdCl(DMPP)] (4)

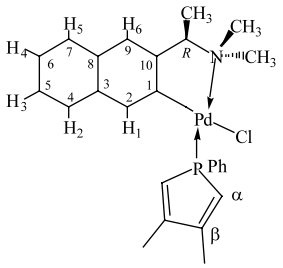

To a suspension of 5.0 g (5.8 mmol) [(*R*)-(2TMNA)PdCl]$_2$ [25b] in 50 mL CH_2Cl_2 was added 2.8 g (14.7 mmol) DMPP. The clear, light orange, solution was stirred at ambient temperature for 10 h, reduced in volume to ca. 10 mL, and *n*-hexane was added to produce a pale yellow solid. The solid was isolated by filtration, washed with *n*-hexane and diethyl ether and recrystallized from CH_2Cl_2–*n*-hexane/diethyl ether to yield 7.33 g (94.5%) of the product as pale yellow prisms m.p. 186–188 °C; $[\alpha]_D = -52.0$ (C, 0.2, CH_2Cl_2). CD (molecular elipticity $[\theta]_\lambda$ (deg cm^2 d mol^{-1}) for $c = 1.23 \times 10^{-4}$ M in CH_2Cl_2 at 25 °C) $[\theta]_{404} = 0$, $[\theta]_{338} = -7120$, $[\theta]_{302} = -5900$, $[\theta]_{290} = 0$, $[\theta]_{272} = +13800$, $[\theta]_{247} = +13400$, $[\theta]_{239} = 0$, $[\theta]_{233} = -17900$. Anal. Calc. for $C_{26}H_{29}ClNPPd$: C, 59.13; H, 5.49; Cl, 6.71. Found: C, 59.21; H, 5.30; Cl, 6.56%. ^{1}H-NMR: δ 7.97 (m, 2H, H_o), 7.68 (dd, $^3J(H_2H_3) = 8.0$ Hz, $^4J(H_2H_4) = 1.5$ Hz, 1H, H_2), 7.45 (s, H_6), 7.42 (m, 3H, H_{mp}), 7.41 (dd, $^3J(H_4H_5) = 8.0$ Hz, $^4J(H_3H_5) = 1.5$ Hz, 1H, H_5), 7.33 (ddd, $^3J(H_2H_3) = 8.0$ Hz, $^3J(H_3H_4) = 7.0$ Hz, $^4J(H_3H_5) = 1.5$ Hz, 1H, H_3), 7.33 (d, $^4J(PH) = 6.5$ Hz, 1H, H_1), 7.30 (ddd, $^3J(H_4H_5) = 8.0$ Hz, $^3J(H_3H_4) = 7.0$ Hz, $^4J(H_2H_4) = 1.5$ Hz, 1H, H_4), 6.78 (d, $^2J(PH) = 32.0$ Hz, 1H, H_α), 6.68 (d, $^2J(PH) = 32.5$ Hz, 1H, H_α) 4.01 (q d, $^3J(HH) = 6.5$ Hz, $^4J(PH) = 2.0$ Hz, 1H, CH), 2.87 (d, $^4J(PH) = 2.0$ Hz, 3H, N CH_3), 2.72 (d, $^4J(PH) = 3.0$ Hz, 3H, N CH_3), 2.09 (s, 3H, DMPP–CH_3), 2.08 (s, 3H, DMPP–CH_3), 1.71 (d, $^3J(HH) = 6.5$ Hz, 3H, CCH_3). $^{13}C\{^1H\}$-NMR: δ 152.77 (d, $^2J(PC) = 1.8$ Hz, C_1), 152.42 (d, $^2J(PC) = 11.1$ Hz, C_β), 151.57 (d, $^2J(PC) = 11.7$ Hz, C_β), 146.88 (d, $^3J(PC) = 2.8$ Hz, C_{10}), 135.43 (d, $^2J(PC) = 12.9$ Hz, C_2), 133.85 (d, $^2J(PC) = 12.8$ Hz, C_o), 132.11 (d, $^4J(PC) = 6.2$ Hz, C_3), 131.15 (s, C_8), 130.96 (d, $^4J(PC) = 2.5$ Hz, C_p), 128.73 (d, $^3J(PC) = 11.1$ Hz, C_m), 127.13 (s, C_4), 126.71 (d, $^1J(PC) = 46.9$ Hz, C_i), 126.67 (s, C_7), 126.61 (d, $^1J(PC) = 52.7$ Hz, C_α), 125.74 (d, $^1J(PC) = 52.2$ Hz, C_α), 125.17 (s, C_6), 124.69 (s, C_5), 120.96 (s, C_9), 74.12 (d, $^3J(PC) = 3.1$ Hz, CH), 49.82 (d, $^3J(PC) = 2.9$ Hz, N CH_3), 45.23 (d, $^3J(PC) = 2.3$ Hz, N CH_3), 19.52 (s, C CH_3), 17.75 (d, $^3J(PC) = 2.6$ Hz, DMPP–CH_3), 17.65 (d, $^3J(PC) = 2.6$ Hz, DMPP–CH_3). $^{31}P\{^1H\}$-NMR: δ 37.3.

2.2.5. {(S)-(TMBA)Pd(DMPP)(Cy_2AsVy)[4 + 2]}ClO_4 (5)

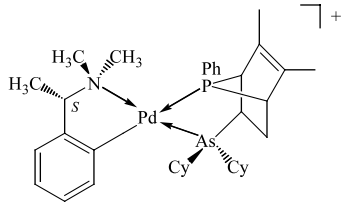

To a solution containing 1.78 g (3.7 mmol) of [(*S*)-(TMBA)PdCl(DMPP)] (**2**), in 25 mL CH_2Cl_2 was added a solution containing 0.77 g (3.7 mmol) of $AgClO_4$ in 1 mL H_2O and 5 mL of acetone. The resulting mixture was stirred in the dark at ambient temperature for 2 h, and then filtered through Celite to remove AgCl. To the filtrate was added 1 g (3.7 mmol) of Cy_2AsVy and the mixture was stirred at ambient temperature for one week. Evaporation to dryness, followed by crystallization from CH_2Cl_2–diethyl ether, afforded 2.6 g (86.7%) of a yellow–brown gum. This material could not be purified by fractional crystallization or column chromatography on silica with a variety of solvents. It was characterized only by $^{31}P\{^1H\}$-NMR spectroscopy: δ 120.13:119.58:119.34:118.42: with a 1:2:6:8 ratio (four diastereomeric Diels–Alder adducts).

2.2.6. {(S)-(1TMNA)Pd(DMPP)(Cy_2AsVy)-[4 + 2]}$C1O_4$ (6)

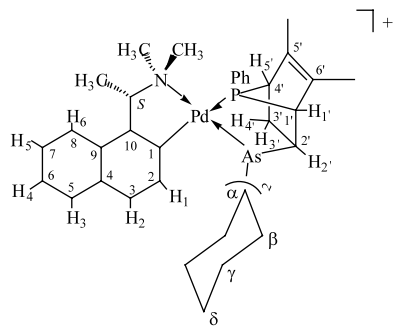

To a solution of 3.14 g (5.9 mmol) of [(*S*)-(1TMNA)PdCl(DMPP)] (**3**), in 50 mL CH_2Cl_2 was added a solution of 1.23 g (6 mmol) $AgClO_4$ in 2 mL H_2O and 10 mL acetone. The resulting mixture was stirred in the dark at ambient temperature for 2 h, and then filtered through celite to remove AgCl. To the filtrate was added 1.6 g (6 mmol) Cy_2AsVy and the mixture was stirred at ambient temperature for one week. Evaporation to dryness followed by crystallization from CH_2Cl_2–diethyl ether afforded 4.95 g (96%) of colorless crystals that were shown by $^{31}P\{^1H\}$-NMR spectroscopy to be a 1:14 mixture of the derived diastereomers δ 119.22, 118.02. Recrystallization of the mixture from CH_2Cl_2–diethyl ether afforded 4.34 g (84%) of the major diastereomer as almost colorless crystals having m.p. 194–196 °C; $[\alpha]_D = +101.0°$ (*c* 0.2, CH_2Cl_2). CD (molecular elipticity $[\theta]_\lambda$ (deg cm^2 d mol^{-1}) for $c = 2.39 \times 10^{-4}$ M in CH_2Cl_2 at 25 °C) $[\theta]_{519} = -6173$, $[\theta]_{390} = 0$, $[\theta]_{343} = +3675$, $[\theta]_{329} = 0$, $[\theta]_{321} = -111$, $[\theta]_{317} = 0$, $[\theta]_{308} = +4189$, $[\theta]_{259} = +77786$. Anal. Calc. for $C_{40}H_{54}AsClNO_4PPd$: C, 55.79; H, 6.27; Cl, 4.02. Found: C, 55.58; H, 6.40; Cl, 4.01%. ^{1}H-NMR: δ 7.79 (dd, $^3J(H_3H_4) = 7.0$ Hz, $^4J(H_3H_5) = 1.5$ Hz, 1H, H_3), 7.68 (dd, $^3J(H_5H_6) = 7.0$ Hz, $^4J(H_4H_6) = 1.0$ Hz, 1H, H_6), 7.50 (m, 6H, H_2, $H_{o,m,p}$), 7.42 (apparent td, $^3J(H_4H_5) = {}^3J(H_5H_6) = 7.0$ Hz, $^4J(H_3H_5) = 1.5$ Hz, 1H, H_5), 7.39 (apparent td, $^3J(H_3H_4) = {}^3J(H_4H_5) = 7.0$ Hz, $^4J(H_4H_6) = 1.0$ Hz, 1H, H_4), 7.21 (dd, $^3J(H_1H_2) = 8.5$ Hz, $^4J(PH) = 6.5$ Hz, 1H, H_1), 4,32 (q, $^3J(HH) = 6.5$ Hz, 1H, CH), 3.65 (s, 1H, H_5), 3.01 (d, $^3J(H_{1'}H_{5'}) = 1.5$ Hz, 1H, $H_{1'}$), 2.84 (apparent ddt, $^3J(PH) = 39.5$ Hz, $^3J(H_{2'}H_{4'}) = 9.3$ Hz, $^3J(H_{1'}H_{2'}) = {}^3J(H_{2'}H_{4'}) = 1.5$ Hz, 1H, $H_{2'}$), 2.74 (apparent tt, $^3J(HH) = {}^3J(HH) = 12.5$ Hz, $^3J(HH) = {}^3J(HH) = 2.5$ Hz, 1H, H_α), 2.54 (apparent tt, $^3J(HH) = {}^3J(HH) = 13.0$ Hz, $^3J(HH) = {}^3J(HH) = 3.0$ Hz, 1H, $H_{\alpha a}$), 2.52 (d, $^4J(PH) = 4.5$ Hz, 3H, N CH_3), 2.52 (dd, $^2J(H_{3'}H_{4'}) = 13.5$ Hz, $^3J(H_{2'}H_{3'}) = 1.5$ Hz, 1H, $H_{3'}$), 2.41 (s, 3H, N CH_3), 2.26 (dd, $^2J(HH) = 12.0$ Hz, $^3J(HH) = 3.0$ Hz, 2H, $H_{\beta e}$), 2.14 (dd, $^2J(HH) = 13.5$ Hz, $^3J(HH) = 3.0$ Hz, 2H, $H_{\beta e}$), 2.08 (ddd, $^3J(PH) = 24.5$ Hz, $^2J(H_{3'}H_{4'}) = 13.5$ Hz, $^3J(H_{2'}H_{4'}) = 9.3$ Hz, 1H, $H_{4'}$), 1.98 (m, 2H, $H_{\beta a}$), 1.84 (m, 2H, $H_{\beta a}$), 1.82 (d, $^3J(HH) = 6.5$ Hz, 3H, $CHCH_3$), 1.78 (d, $^4J(PH) = 1.0$ Hz, 3H, C=C CH_3), 1.69 (apparent q d, $^2J(HH) = {}^3J(HH) = {}^3J(HH) = 13.0$ Hz, $^3J(HH) = 3.0$ Hz, 2H, H_γ), 1.59 (m, 2H, H_γ), 1.54 (s, 3H, C=C CH_3), 1.42 (apparent q t, $^2J(HH) = {}^3J(HH) = {}^3J(HH) = 12.5$ Hz, $^3J(HH) = {}^3J(HH) = 3.5$ Hz, 1H, H_δ), 1.35 (apparent q t, $^2J(HH) = {}^3J(HH) = {}^3J(HH) = 12.5$ Hz, $^3J(HH) = {}^3J(HH) = 3.5$ Hz, 1H, H_δ), 1.11 (apparent q t, $^2J(HH) = {}^3J(HH) = {}^3J(HH) = 12.5$ Hz, $^3J(HH) = {}^3J(HH) = 3.0$ Hz, 1H, H_δ), 1.04 (apparent q t, $^2J(HH) = {}^3J(HH) = {}^3J(HH) = 12.5$ Hz, $^3J(HH) = {}^3J(HH) = 3.0$ Hz, 1H, H_δ). $^{13}C\{^1H\}$-NMR: 156.59 (d, $^2J(PC) = 113$ Hz, C_1), 151.29 ($C_{5'}$ or $C_{6'}$), 136.22 (d, $^3J(PC) = 3.4$ Hz, C_2), 135.73 (d, $^2J(PC) = 3.1$ Hz, $C_{6'}$ or $C_{5'}$), 132.26 (d, $^2J(PC) = 10.4$ Hz, C_o), 131.83 (C_9), 131.23 (d, $^4J(PC) = 1.5$ Hz, C_p), 131.23 (d, $^1J(PC) = 52.3$ Hz, C_i), 129.23 (d, $^3J(PC) = 8.9$ Hz, C_m), 129.21 (d, $^3J(PC) = 6.2$ Hz, C_{10}), 128.73 (C_4), 128.24 (C_5), 126.30 (C_6), 125.90 (d, $^4J(PC) = 7.9$ Hz, C_3), 124.90 (C_7), 123.60 (C_8), 75.83 (d, $^3J(PC) = 4.4$ Hz, CH), 55.37 (d, $^1J(PC) = 28.5$ Hz, $C_{1'}$), 51.84 (N CH_3), 47.26 (d, $^1J(PC) = 19.6$ Hz, $C_{4'}$), 39.49 (N CH_3), 38.64 (C_α), 34.27 (C_α), 32.38 (C_β), 32.12 (C_β), 31.79 (C_β), 31.43 (d, $^2J(PC) = 18.7$ Hz, $C_{3'}$), 29.52 (d, $^2J(PC) = 38.9$ Hz, $C_{2'}$), 28.24 (C_γ), 27.99 (C_γ) 27.60 (C_γ), 27.59 (C_γ), 25.80 (C_δ), 25.55 (C_δ), 25.03 (C CH_3), 14.56 (d, $^3J(PC) = 2.5$ Hz, C=C CH_3), 13.48 (d, $^3J(PC) = 2.0$ Hz, C=C CH_3). $^{31}P\{^1H\}$-NMR: δ 118.08.

2.2.7. *{(R)-(2TMNA)Pd(DMPP)(Cy_2AsVy)-[4 + 2]}ClO_4 (7)*

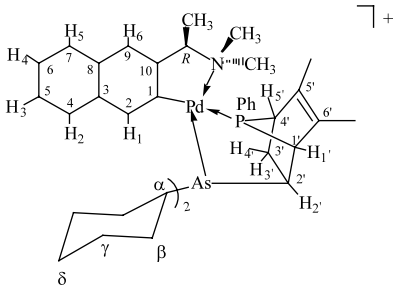

To a solution of 5.28 g (10^{-2} mol) of [(*R*)-(2TMNA)PdCl(DMPP)] (**4**), in 100 mL CH_2Cl_2 was added a solution of 2.07 g (10^{-2} mol) $AgClO_4$ in 5 mL H_2O and 15 mL acetone. The resulting mixture was stirred in the dark at ambient temperature for 2 h, and then filtered through celite to remove AgCl. To the filtrate was added 2.68 g (10^{-2} mol) Cy_2AsVy and the mixture was stirred at ambient temperature for 4 days. Evaporation of the solution to dryness on a rotary evaporator, followed by crystallization of the residue from CH_3OH–diethyl ether–*n*-hexane afforded 9.91 g (92%) of white microcrystals that were shown by $^{31}P\{^1H\}$-NMR spectroscopy to be a 1:6 mixture of the diastereomeric product. δ $^{31}P = 119.86$, 118.74 ppm. Recrystallization of the mixture from CH_2Cl_2–CH_3OH–diethyl ether afforded 4.8 g (55.8%) of the major diastereomer as colorless needles having m.p. 210–212 °C (dec.): $[\alpha]_D = -11.0°$ (*c* 0.2, CH_2Cl_2). CD (molecular elipticity $[\theta]_\lambda$ (deg cm^2 d mol^{-1}) for $c = 1.4 \times 10^{-3}$ M in CH_2Cl_2 at 25 °C) $[\theta]_{229} = +49800$, $[\theta]_{280\ sh} = +22800$, $[\theta]_{270} = 0$, $[\theta]_{255} = -76800$, $[\theta]_{231} = -212000$. Anal. Calc. For $C_{40}H_{54}AsClO_4PPd$: C, 55.79; H, 6.27; Cl, 4.02. Found: C, 55.58; H, 6.31; Cl, 3.79%. ^{1}H-NMR: δ 7.70 (dd, $^3J(H_2H_3) = 8.0$ Hz, $^4J(H_2H_4) = 1.5$ Hz, 1H, H_2), 7.68 (dd, $^3J(H_4H_5) = 8.0$ Hz, $^4J(H_3H_5) = 1.5$ Hz, 1H, H_5), 7.56 (d, $^4J(PH) = 2.0$ Hz, 1H, H_1), 7.50 (s, 1H, H_6), 7.48 (m, 5H, H_o, m.p.),

7.41 (ddd, $^3J(H_2H_3) = 8.0$ Hz, $^3J(H_3H_4) = 7.0$ Hz, $^4J(H_3H_5) = 1.5$ Hz, 1H, H_3), 7.37 (ddd, $^3J(H_4H_5) = 8.0$ Hz, $^3J(H_3H_4) = 7.0$ Hz, $^4J(H_2H_4) = 1.5$ Hz, 1H, H_4), 3.64 (apparent t, $^3J(H_{3'}H_{5'}) = {}^4J(H_{1'}H_{5'}) = 1.5$ Hz, 1H, $H_{5'}$), 3.59 (q, $^3J(HH) = 6.5$ Hz, 1H, CH), 3.01 (apparent q, $^3J(H_{1'}H_{2'}) = {}^3J(H_{1'}H_{5'}) = {}^2J(PH) = 1.5$ Hz, 1H, $H_{1'}$), 2.87 (apparent ddt, $^3J(PH) = 41.5$ Hz, $^3J(H_{2'}H_{4'}) = 9.0$ Hz, $^3J(H_{2'}H_{3'}) = {}^3J(H_{1'}H_{2'}) = 1.5$ Hz, 1H, $H_{2'}$), 2.8 (tt, $^3J(HH) = {}^3J(HH) = 12.5$ Hz, $^3J(HH) = {}^3J(HH) = 3.0$ Hz, 1H, $H_{\alpha a}$), 2.61 (tt, $^3J(HH) = {}^3J(HH) = 12.5$ Hz, $^3J(HH) = {}^3J(HH) = 3.0$ Hz, 1H, $H_{\alpha a}$), 2.52 (apparent dt, $^2J(H_{3'}H_{4'}) = 13.0$ Hz, $^3J(H_{2'}H_{3'}) = {}^3J(H_{3'}H_{5'}) = 1.5$ Hz, 1H, $H_{3'}$), 2.45 (d, $^4J(PH) = 2.0$ Hz, 3H, N CH_3), 2.32 (s, 3H, N CH_3), 2.26 (dd, $^2J(HH) = 12.0$ Hz, $^3J(HH) = 3.0$ Hz, 2H, $H_{\beta e}$), 2.18 (dd, $^2J(HH) = 12.5$ Hz, $^3J(HH) = 3.0$ Hz, 2H, $H_{\beta e}$), 2.08 (ddd, $^3J(PH) = 25.0$ Hz, $^2J(H_{3'}H_{4'}) = 13.0$ Hz, $^3J(H_{2'}H_{4'}) = 9.0$ Hz, 1H, $H_{4'}$), 2.00 (m, 2H, $H_{\beta a}$), 1.80 (m, 2H, $H_{\beta a}$), 1.76 (d, $^4J(PH) = 1.0$ Hz, 3H, C=C CH_3), 1.74 (d, $^3J(HH) = 6.5$ Hz, 3H, $CHCH_3$), 1.68 (m, 2H, H_γ), 1.58 (m, 4H, H_γ), 1.48 (m, 2H, H_γ), 1.38 (apparent qt, $^2J(HH) = {}^3J(HH) = {}^3J(HH) = 13.5$ Hz, $^3J(HH) = {}^3J(HH) = 3.0$ Hz, 1H, H_δ), 1.35 (apparent qt, $^2J(HH) = {}^3J(HH) = {}^3J(HH) = 13.5$ Hz, $^3J(HH) = {}^3J(HH) = 3.0$ Hz, 1H, H_δ), 1.10 (apparent qt, $^2J(HH) = {}^3J(HH) = {}^3J(HH) = 13.5$ Hz, $^3J(HH) = {}^3J(HH) = 3.0$ Hz, 1H, H_δ), 1.06 (apparent qt, $^2J(HH) = {}^3J(HH) = {}^3J(HH) = 13.5$ Hz, $^3J(HH) = {}^3J(HH) = 3.0$ Hz, 1H, H_δ). $^{13}C\{^1H\}$-NMR: δ 155.23 (d, $^2J(PC) = 113$ Hz, C_1), 154.0 ($C_{5'}$ or $C_{6'}$), 137.21 (d, $^4J(PC) = 2.5$ Hz, C_9), 135.39 (d, $^3J(PC) = 3.1$ Hz, C_{10}), 132.09 (d, $^2J(PC) = 10.3$ Hz, C_o), 131.99 (d, $^4J(PC) = 8.8$ Hz, C_3), 131.74 (s, C_8), 131.08 (s, C_p), 129.20 (d, $^3J(PC) = 8.8$ Hz, C_m), 128.26 ($C_{5'}$ or $C_{6'}$), 127.59 (d, $^1J(PC) = 23.0$ Hz, C_i), 127.18 (s, C_4), 127.10 (s, C_7), 125.40 (s, C_5), 125.14 (s, C_6), 120.48 (d, $^3J(PC) = 5.3$ Hz, C_2), 78.12 (d, $^4J(PC) = 3.3$ Hz, CH), 55.18 (d, $^1J(PC) = 28.9$ Hz, $C_{1'}$), 51.22 (s, N CH_3), 50.18 (d, $^3J(PC) = 4.9$ Hz, N CH_3), 47.13 (d, $^1J(PC) = 19.9$ Hz, $C_{4'}$), 39.20 (C_α), 38.51 (C_α), 34.00 (C_β), 32.34 (C_β), 32.01

Table 1
Crystallographic data for complexes **3**, **6b**, **7b**, **8b**, **9b** and **11**

	3	**6b**	**7b**	**8b**	**9b**	**11**
Chemical formula	$C_{26}H_{29}ClNPPdCl\cdot0.333(C_7H_8)\cdot0.273\ (CHCl_3)$	$C_{40}H_{54}AsNPPd(ClO_4)\cdot0.225(CH_2Cl_2)$	$C_{40}H_{54}AsNPPd(ClO_4)\cdot0.6\ CH_2Cl_2\cdot0.4CH_3OH$	$C_{26}H_{38}AsCl_2PPd\cdot CH_2Cl_2$	$C_{33}H_{46}AsClPRu + PF_6^-\cdot CH_2Cl_2$	$C_{16}H_{20}Cl_3Ru_2 + PF6^-$
Formula weight	591.68	879.73	924.40	718.72	915.04	665.80
Crystal size (mm)	$0.23\times0.20\times0.10$	$0.30\times0.06\times0.04$	$0.33\times0.20\times0.15$	$0.30\times0.16\times0.03$	$0.20\times0.20\times0.20$	$0.26\times0.14\times0.03$
Space group	$R\bar{3}$	$P2_12_12_1$	$P2_12_12_1$	$P2_12_12_1$	$P2_12_12_1$	$P2_1/a$
Unit cell dimensions						
a (Å)	25.9655(3)	10.3395(1)	10.6280(1)	10.1853(1)	12.1679(1)	10.6399(1)
b (Å)	25.9655(3)	13.7179(2)	13.9690(1)	11.7903(1)	14.5174(1)	18.4496(2)
c (Å)	10.87620(10)	30.5848(4)	29.6497(2)	25.3267(3)	21.4051(2)	10.9676(2)
α (°)	90	90	90	90	90	90
β (°)	90	90	90	90	90	94.5036(5)
γ (°)	120	90	90	90	90	90
V (Å^3)	6350.40(12)	4338.03(8)	4401.87(5)	3041.43(5)	3781.13(5)	2146.31(4)
Z	9	4	4	4	4	4
D_{calc} (g cm^{-3})	1.392	1.347	1.395	1.569	1.607	2.060
μ (mm^{-1})	0.903	1.348	1.377	2.109	1.634	1.906
Reflections Collected	70695	60057	210055	74129	78750	64180
Unique reflections	8292	7617	12834	7438	11072	4110
Max/min transmission factors	0.926/0.812	0.950/0.811	0.876/0.735	0.939/0.586	0.779/0.753	0.946/0.667
Data/restraints/parameters	8046/0/297	6287/0/455	9823/0/468	7438/0/317	8685/0/424	4110/0/253
Goodness-of-fit	1.59	1.407	1.966	1.389	1.610	1.957
Flack parameter	0.00(2)	0.001(1)	0.001(1)	0.001(1)	0.001(1)	–
R_1/wR_2 ($I>2\sigma(I)$) [a]	0.031/0.041	0.036/0.0385	0.0437/0.0481	0.0351/0.0368	0.0388/0.0415	0.0505/0.0732

[a] $R_1 = \Sigma\|\|F_o|-|F_c\|/\Sigma F_o$, $wR_2 = \{\Sigma[w(|F_o|-|F_c|)^2]/\Sigma w(F_o)^2\}^{0.5}$, $w = 1/[\sigma^2(F_o)+a|F_o|^2]$, (**3**) $a = 0.004$, (**6b**–**9b**) $a = 0.00022$.

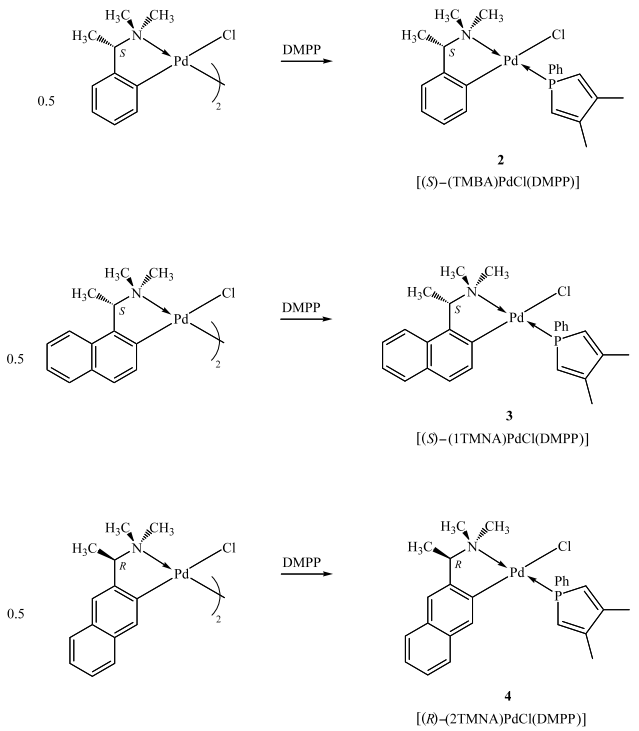

Scheme 1.

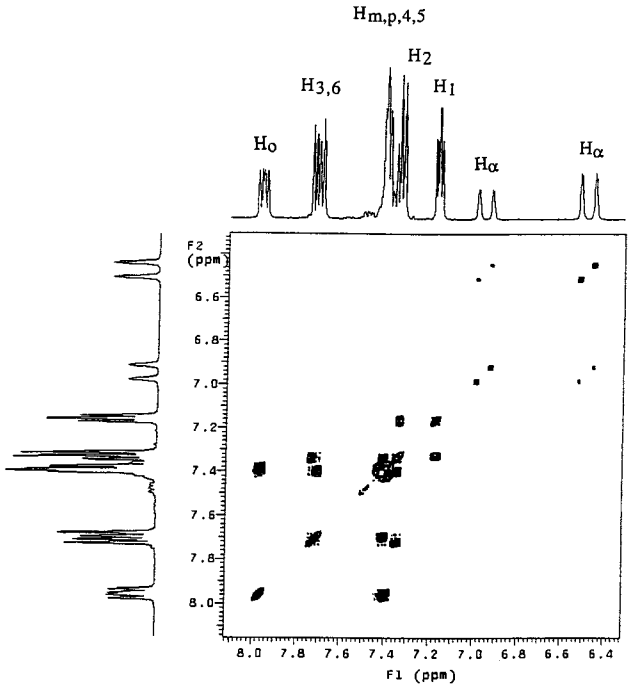

Fig. 1. Expansion of the 500 MHz COSY spectrum of **3** in the low field region.

(C_β), 31.95 (C_β), 31.30 (d, $^2J(PC) = 18.2$ Hz, $C_{3'}$), 29.6 (d, $^2J(PC) = 39.1$ Hz, $C_{2'}$), 28.22 (C_γ), 27.95 (C_γ), 27.45 (C_γ), 25.83 C CH_3), 25.70 (C_δ), 25.45 (C_δ), 14.44 (d, $^3J(PC) = 2.4$ Hz, C=C CH_3), 13.35 (d, $^3J(PC) = 1.6$ Hz, C=C CH_3). $^{31}P\{^1H\}$-NMR: δ 118.74.

2.2.8. (−)-{$PdCl_2$(DMPP)(Cy_2AsVy)[4 + 2]} (**8b**)

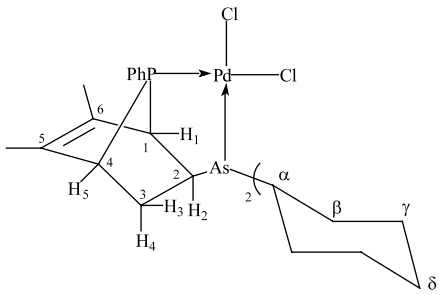

To a solution containing 3.5 g (4.1 mmol) of **6b** in 50 mL CH_2Cl_2 was added 10 mL of 12 M HCl and 50 mL acetone. This mixture was stirred at ambient temperature for 2 days, the CH_2Cl_2 layer was separated and the solvent was removed on a rotary evaporator. The pale yellow solid that remained was washed with H_2O, ethanol and diethyl ether and recrystallized from CH_2Cl_2–*n*-hexane to afford 2.4 g (93%) of pale yellow crystals having m.p. 240–242 °C. $[\alpha]_D = -35.5°$ (*c* 0.2, CH_2Cl_2). CD (molecular elipticity $[\theta]_\lambda$ (deg cm^2 d mol^{-1}) for $c = 3.15 \times 10^{-3}$ M in CH_2Cl_2 at 25 °C) $[\theta]_{384} = +2100$, $[\theta]_{370} = 0$, $[\theta]_{322} = -16{,}600$, $[\theta]_{300} = 0$, $[\theta]_{292\ sh} = +12{,}500$, $[\theta]_{262} = +45400$. Anal. Calc. for $C_{26}H_{38}AsCl_2PPd \cdot CH_2Cl_2$: C, 45.14; H, 5.57; Cl, 19.74. Found: C, 45.01; H, 5.26; Cl, 19.66%. ^{1}H-NMR: δ 7.51 (m, 2H, H_o), 7.45 (m, 1H, H_p), 7.40 (m, 2H, H_m), 3.30 (dd, $^4J(H_1H_5) = 2.0$ Hz, $^3J(H_3H_5) = 1.5$ Hz, 1H, H_5), 3.06 (apparent t, $^2J(PH) = {}^4J(H_1H_5) = 2.0$ Hz, 1H, H_1), 2.89 (apparent tt, $^3J(HH) = {}^3J(HH) = 13.0$ Hz, $^3J(HH) = {}^3J(HH) = 3.0$ Hz, 1H, $H_{\alpha a}$), 2.62 (dd,

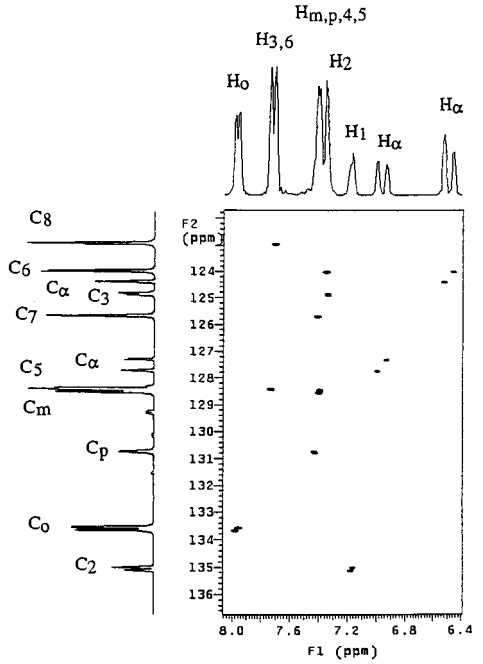

Fig. 2. Expansion of the 125 MHz HETCOR spectrum of **3** in the low field region.

^3J(PH) = 31.0 Hz, $^3J(H_2H_4)$ = 9.3 Hz, 1H, H_2), 2.60 (dd, ^2J(HH) = 12.0 Hz, ^3J(HH) = 3.0 Hz, 1H, $H_{\beta e}$), 2.57 (apparent tt, ^3J(HH) = 13.0 Hz, ^3J(HH) = 3.0 Hz, 1H, $H_{\alpha a}$), 2.49 (dd, $^2J(H_3H_4)$ = 13.0 Hz, $^3J(H_3H_5)$ = 1.5 Hz, 1H, H_3), 2.43 (dd, ^2J(HH) = 13.0 Hz, ^3J(HH) = 3.0 Hz, 1H, $H_{\beta e}$), 2.36 (dd, ^2J(HH) = 13.0 Hz, ^3J(HH) = 3.0 Hz, 1H, $H_{\beta e}$), 2.27 (dd, ^2J(HH) = 13.0 Hz, ^3J(HH) = 3.0 Hz, 1H, $H_{\beta e}$), 1.94 (ddd, ^3J(PH) = 24.0 Hz, $^2J(H_3H_4)$ = 13.0 Hz, $^3J(H_2H_4)$ = 9.3 Hz, 1H, H_4), 1.84 (m, 8H, 2 H_β, 4 H_γ, 2 H_δ), 1.64 (apparent q d, ^2J(HH) = ^3J(HH) = ^3J(HH) = 13.0 Hz, ^3J(HH) = 3.0 Hz, 1H, $H_{\beta a}$), 1.58 (apparent q d, ^2J(HH) = ^3J(HH) = ^3J(HH) = 13.0 Hz, ^3J(HH) = 3.0 Hz, 1H, $H_{\beta a}$), 1.58 (s, 3H, CH_3), 1.52 (s, 3H, CH_3), 1.38 (m, 4H, H_γ), 1.29 (apparent q t, ^2J(HH) = ^3J(HH) = ^3J(HH) = 13.0 Hz, ^3J(HH) = 3.0 Hz, 1H, H_δ), 1.24 (apparent q t, ^2J(HH) = ^3J(HH) = ^3J(HH) = 13.0 Hz, 1H, H_δ). $^{13}C\{^1H\}$-NMR: δ 135.78 (C_5), 132.50 (d, ^2J(PC) = 9.3 Hz, C_o), 131.22 (d, ^4J(PC) = 2.4 Hz, C_p), 129.00 (d, ^2J(PC) = 1.9 Hz, C_6), 128.16 (d, ^3J(PC) = 11.1 Hz, C_m), 125.69 (d, ^1J(PC) = 47.8 Hz, C_i), 55.57 (d, ^1J(PC) = 35.0 Hz, C_1), 47.48 (d, ^1J(PC) = 29.3 Hz, C_4), 40.46 (C_α), 39.53 (C_α), 32.23 (C_β), 32.19 (C_β), 31.58 (C_β), 31.09 (d, ^2J(PC) = 16.6 Hz, C_3), 30.84 (C_β), 28.01 (C_γ), 27.79 (C_γ), 27.66 (C_γ), 27.39 (C_γ), 26.71 (d, ^2J(PC) = 40.1 Hz, C_2), 25.86 (C_δ), 25.68 (C_δ), 14.95 (d, ^3J(PC) = 2.6 Hz, CH_3), 13.62 (d, ^3J(PC) = 3.0 Hz, CH_3). $^{31}P\{^1H\}$-NMR: δ 130.87.

2.2.9. *{(η^6-$H_3CC_6H_5$)Ru[(DMPP)(Cy_2AsCVy)-[4 + 2]Cl}PF_6* (**9**)

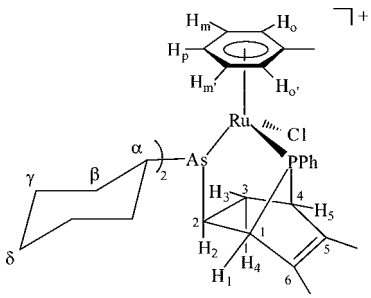

To a solution containing 1 g (1.4 mmol) of **8b** in 100 mL CH_2Cl_2 was added a solution containing 9 g (0.18 mol) NaCN in 100 mL H_2O. The mixture was stirred vigorously for 4 h. The CH_2Cl_2 layer was separated, dried over anhydrous Na_2SO_4, and 0.367 g (0.7 mmol) [(η^6-$H_3CC_6H_5$)$RuCl_2$]$_2$ and 0.23 g (1.4 mmol) NH_4PF_6 were added. The mixture was stirred at ambient temperature for 16 h. The solvents were removed by rotary evaporation and the residue was crystallized from acetone–diethyl ether to yield 0.98 g (84.5%) of the yellow microcrystalline product that was shown by $^{31}P\{^1H\}$-NMR spectroscopy to be a 1.67:1 ratio of diastereomers: δ 147.92 (1.67 P), 143.50 (1P), −143.13 (sept, ^1J(PF) = 713 Hz, 2.67P, PF_6^-). Recrystallization from CH_2Cl_2–*n*-hexane afforded 0.42 g (36.2%) of the major diastereomer, m.p. > 300 °C dec. $[\alpha]_D$ = −126.8° (*c* 0.2, CH_2Cl_2). CD (molecular elipticity $[\theta]_\lambda$ (deg cm^2 d mol^{-1}) for $c = 1 \times 10^{-3}$ M in CH_2Cl_2 at 25 °C) $[\theta]_{640} = 0$, $[\theta]_{516} = -22200$, $[\theta]_{455} = -25627$, $[\theta]_{328} = -15291$, $[\theta]_{251} = -104460$. Anal. Calc. for $C_{33}H_{46}AsClF_6P_2Ru$: C, 47.77; H, 5.54; Cl, 4.27. Found: C, 47.63; H, 5.29; Cl, 4.14%. ^{1}H-NMR: δ 7.90 (m, 1H, H_oPh), 7.57 (m, 1H, H_oPh), 7.49 (m, 3H, H_{mp}Ph), 5.96 (d, ^3J(HH) = 6.0 Hz, 1H, H_o), 5.74 (t, ^3J(HH) = 6.0 Hz, 1H, H_m), 5.02 (d, ^3J(HH) = 6.0 Hz, 1H, $H_{o'}$), 5.02 (t, ^3J(HH) = 6.0 Hz, 1H, H_p), 4.81 (td, ^3J(HH) = 6.0 Hz, J(PH) = 1.5 Hz, 1H, H_p), 3.13 (b s, 1H, H_1), 3.11 (d, $^3J(H_3H_5)$ = 3.0 Hz, 1H, H_5), 2.87 (apparent tt, ^3J(HH) = ^3J(HH) = 12.5 Hz, ^3J(HH) = ^3J(HH) = 2.5 Hz, 1H, $H_{\alpha a}$), 2.74 (dd, $^2J(H_3H_4)$ = 13.0 Hz, $^3J(H_3H_5)$ = 3.0 Hz, 1H, H_3), 2.61 (dd, ^3J(PH) = 40.5 Hz, $^3J(H_2H_4)$ = 9.3 Hz, 1H, H_2), 2.59 (apparent tt, ^3J(HH) = ^3J(HH) = 13.0 Hz, ^3J(HH) = ^3J(HH) = 2.5 Hz, 1H, $H_{\alpha a}$), 2.08 (s, 3H, tol CH_3), 2.06 − 1.69 (m, 16H, 8 H_β 8 H_γ), 1.64 (s, 3H, CH_3), 2.10 (ddd, ^3J(PH) = 21.0 Hz, $^2J(H_3H_4)$ = 13.0 Hz, $^3J(H_2H_4)$ = 9.3 Hz, 1H, H_4), 1.40 (s, 3H, CH_3), 1.30 (m, 4H, H_δ). ^{13}C $\{^1H\}$-NMR: δ 137.86 (C=C), 132.83 (d, ^1J(PC) = 44.3 Hz, C_i), 131.44 (s, C=C), 131.21 (d, ^2J(PC) = 5.3 Hz, C_o), 130.79 (d, ^4J(PC) = 2.0 Hz, C_p), 129.90 (d, ^3J(PC) = 12.1 Hz, C_m), 129.21 (d, ^2J(PC) = 7.7 Hz, C_o), 128.55 (d, ^3J(PC) = 9.8 Hz C_m), 112.50 (d, J(PC) = 2.9 Hz, arene C_i), 98.21 (s, arene $C_{o'}$), 95.85 (d, J(PC) = 7.4 Hz, arene C_o), 90.53 (s, arene $C_{m'}$), 86.31 (d, J(PC) = 2.3 Hz, arene C_m), 71.72 (s, arene C_p), 54.89 (d, ^1J(PC) = 37.0 Hz, C_1), 48.26 (d, ^1J(PC) = 30.4 Hz, C_4), 41.88 (C_α), 36.34 (C_α), 31.28 (C_β), 31.00 (C_β), 30.56 (C_β), 29.80 (C_β), 28.19 (d, ^2J(PC) = 11.3 Hz, C_3), 27.98 (C_γ), 27.78 (C_γ), 26.73 (C_γ), 26.41 (C_γ), 26.14 (C_δ), 25.91 (C_δ), 25.14 (d, ^2J(PC) = 39.0 Hz, C_2), 18.43 (tol CH_3), 14.88 (d, ^3J(PC) = 2.3 Hz, C=C CH_3), 13.72 (d, ^3J(PC) = 2.3 Hz, C=C CH_3). $^{31}P\{^1H\}$-NMR: δ 147.46 (s, 1P, P_7), −143.131 sept, ^1J(PF) = 713 Hz, 1 P, PF_6^-). The minor diastereomer could not be separated from the major diastereomer; NMR data for it were obtained from the mixture. ^{1}H-NMR: δ 7.70 (m, 1H, H_oPh), 7.59 (m, 1H, H_oPh), 7.42 (m, 1H,H_pPh) 7.35 (m, 2H, H_mPh) 5.29 (d, ^3J(HH) = 5.5 Hz, 1H, H_o), 5.81 (t, ^3J(HH) = 5.5 Hz, 1H, H_m), 5.60 (dd, ^3J(HH) = 6.0 Hz, ^3J(HH) = 5.5 Hz, 1H, H_p), 5.24 (t, ^3J(HH) = 6.0 Hz, 1H, $H_{m'}$), 5.04 (d, ^3J(HH) = 6.0 Hz, 1H, $H_{o'}$), 3.44 (d, ^3J(PH) = 42.0 Hz, 1H, H_2), 3.31 (bs, 1H, H_5), 2.96 (bs, 1H, H_1), 2.91 (tt, ^3J(HH) = ^3J(HH) = 12.5 Hz, ^3J(HH) = ^3J(HH) = 3.0 Hz, 1H, H_α), 2.88 (tt, ^3J(HH) = ^3J(HH) = 12.5 Hz, ^3J(HH) = ^3J(HH) = 3.0 Hz, 1H, H_α), 2.38 (dd, ^3J(PH) = 27.0 Hz, $^2J(H_3H_4)$ = 12.0 Hz, 1H, H_4), 1.82 (d, $^2J(H_3H_4)$ = 12.0 Hz, 1H, H_3), 1.79 (s, 3H, Tol CH_3), 1.48 (s, 3H, C=C CH_3), 1.47 (s, 3H, C=C CH_3). (The remaining cyclo-

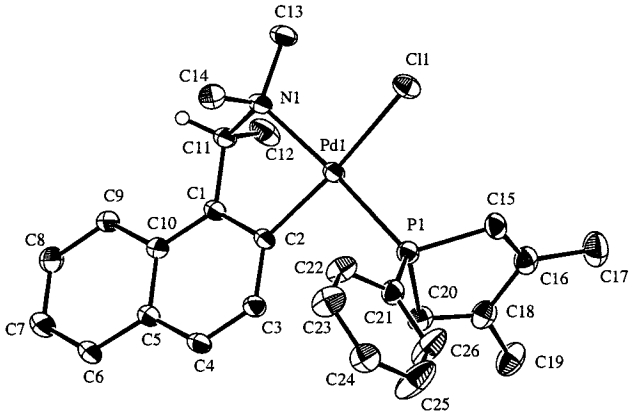

Fig. 3. Structural drawing of **3** showing the atom numbering scheme (30% probability ellipsoids). The hydrogen atom on C(11) has an arbitrary radius.

Table 2
Selected bond distances (Å) and angles (°) for **3** and **4**

Compound	**3**	**4** [a]
Bond distances		
Pd(1)–C(1)/C(2)	2.007(4)	2.08(2)
Pd(1)–C1(1)	2.4123(10)	2.372(7)
Pd(1)–N(1)	2.134(6)	2.20(2)
Pd(1)–P(1)	2.250(14)	2.219(6)
Bond angles		
N(1)–Pd(1)–C(1)/C(2)	81.20(18)	82.8(8)
P(1)–Pd(1)–C(1)/C(2)	92.02(5)	92.2(6)
N(1)–Pd(1)–P(1)	173.47(9)	175.0(6)
Cl(1)–Pd(1)–C(1)/C(2)	172.06(13)	172.5(5)
N(1)–Pd(1)–Cl(1)	93.92(9)	92.6(6)
P(1)–Pd(1)–Cl(1)	93.18(16)	92.4(3)

[a] Ref. [17].

hexyl proton resonances could not be distinguished from those of the major diastereomer). $^{13}C\{^1H\}$-NMR: δ 138.06 (C=C), 132.16 (C=C), 129.70 (d, $^2J(PC) = 5.5$ Hz, C_o), 129.45 (s, C_p), 128.70 (d, $^3J(PC) = 12.5$ Hz, C_m), 128.45 (d, $^2J(PC) = 8.9$ Hz, C_o), 128.12 (d, $^3J(PC) = 9.9$ Hz, C_m), 124.40 (d, $^1J(PC) = 46.4$ Hz, C_i), 111.00 (d, $J(PC) = 2.4$ Hz, arene C_i), 94.52 (d, $J(PC) = 7.0$ Hz, arene C_o), 93.01 (s, arene $C_{o'}$), 90.16 (s, arene $C_{m'}$), 86.54 (s, arene C_p), 51.33 (d, $^1J(PC) = 39.0$ Hz, C_1), 48.16 (d, $^1J(PC) = 30.1$ Hz, C_4), 42.24 (C_α), 36.55 (C_α), 31.06 (C_β), 30.69 (C_β), 30.50 (C_β), 29.48 (C_β), 27.93 (d, $^2J(PC) = 12.3$ Hz, C_3), 27.23 (C_γ), 26.50 (C_γ), 26.20 (C_γ), 26.22 (d, $^2J(PC) = 30.6$ Hz, C_2), 25.88 (C_γ), 25.65 (C_δ), 24.98 (C_δ), 17.87 (tol CH_3), 14.48 (d, $^3J(PC) = 2.9$ Hz, C=C CH_3, 13.40 (d, $^3J(PC) = 2.3$ Hz, C=C CH_3.

*2.2.10. Attempted synthesis of {(p-$H_3CC_6H_4CH_3$)-Ru(DMPP)(Cy_2AsVy)[4 + 2]Cl}PF_6 (**10**)*

As for **9**, the arsinophosphine was displaced by cyanide from 1 g (1.4 mmol) of **8** and reacted with 0.39 g (1.4 mmol) of $[(\eta^6\text{-}p\text{-}H_3CC_6H_4CH_3)RuCl_2]_2$ and 0.23 g (1.4 mmol) of NH_4PF_6. After removal of solvents, the residue was crystallized from acetone–diethyl ether. The yellow–brown residue was shown by ^{1}H-, $^{13}C\{^1H\}$- and $^{31}P\{^1H\}$-NMR spectroscopy to be a mixture of two diastereomers of **10** (2.4:1) (δ ^{31}P, 145.61 and 143.84, respectively) and $[\{(\eta^6\text{-}p\text{-}H_3CC_6H_4CH_3)Ru\}_2\mu\text{-}(Cl)_3]PF_6$ (**11**), Compound **11** was isolated by fractional crystallization from CH_2Cl_2–*n*-hexane and recrystallized from acetone–diethyl ether to afford 0.12 g of brownish-yellow plates m.p. 208–212 °C, (dec.). Anal. Calc. for $C_{16}H_{20}Cl_3F_6PRu_2$: C, 28.87; H, 3.00; Cl, 15.98. Found: C, 28.69; H, 3.07; Cl, 15.75%. ^{1}H-NMR (acetone-d_6) δ 5.84 (s, 8H, arene CH), 2.20 (s, 12H, CH_3). $^{13}C\{^1H\}$-NMR: δ 95.32 (arene C_i), 80.59 (arene CH), 18.72 (CH_3). $^{31}P\{^1H\}$-NMR: δ −144.30 (sept, $^1J(PF) = 706$ Hz, PF_6^-).

2.3. X-ray data collection and processing

Crystals of the compounds were obtained from CH_2Cl_2–*n*-hexane (**6b**, **7b**, **8b**, **9b**, **11**) or toluene–$CHCl_3$–*n*-hexane (**3**) mixtures, mounted on glass fibers and placed on a Nonius Kappa CCD diffractometer. Intensity data were taken in the ϕ and ω modes with Mo–K_α graphite monochromated radiation ($\lambda = 0.7107$ Å) at 200 K. The data were corrected for Lorentz, polarization effects, and absorption by integration using the Gaussian method [29]. Scattering factors and corrections for anomalous dispersion were taken from a standard source [30]. Calculations were performed with the TEXSAN (MSC 1992–1997) software package Version 1.8 on the Silicon Graphics Power Challenge computer of the Australian National University's supercomputer facility. The structures were solved by Patterson methods. Anisotropic thermal parameters were assigned to all non-hydrogen atoms. Hydrogen atoms were included at calculated positions in which the C–H vector was fixed at 0.95 Å but not refined. Compounds **6b**, **7b**, **8b**, and **9b** crystallized as solvates. The absolute configurations of the complexes were determined by refinement of the Flack parameters [31], and were consistent with the known configurations of the carbon stereocenters in the amine components of the compounds. Crystallographic data are given in Table 1.

3. Results and discussion

As indicated in Scheme 1, like many other ligands [16,17,32], DMPP readily cleaves the chloride bridges of dimeric orthopalladated amine complexes in a regioselective manner to form complexes **2**–**4**. The regioselectivity of the ligand substitution reactions was readily established by NMR spectroscopy. Complete assignments of all proton and carbon chemical shifts were made with the aid of APT, COSY, and HETCOR

spectra. Typical COSY and HETCOR spectra are shown in Figs. 1 and 2, respectively. Because the complexes are devoid of symmetry, the CH_3 and αCH groups of the phosphole are each diastereotopic. The two proton resonances for the phosphole CH_3 groups were readily distinguished from those of the NCH_3 and $CHCH_3$ groups by observation of ^4J(HH) couplings between the αCH protons and the phosphole methyl protons. The resonances due to the $CHCH_3$ moiety were readily assigned by the observation of ^3J(HH) coupling between the two proton types. The phosphole αCH resonances were assigned by the observation of large ^2J(PH) couplings, together with the smaller ^4J(HH) allylic coupling and their mutual ^4J(HH) couplings. The remaining ^{1}H resonances in the low-field region divide into separate tightly coupled spin sets comprising the P-phenyl protons and the naphthyl protons. These spin sets were distinguished, one from another, by their mutual couplings and their PH couplings. The P–H coupling interactions were affirmed by ^{1}H{^{31}P} experiments. Once the proton NMR spectra were fully assigned, the ^{13}C{^{1}H}-NMR spectra could then be assigned from the APT and HETCOR spectra (Fig. 2). The ^{31}P{^{1}H}-NMR spectrum of each complex contains one singlet resonance (δ 37.8, **2**, δ 37.3, **3** or **4**) the chemical shift of which is, within experimental error, unaffected by the structure of the amine. The ^{1}H- and ^{13}C{^{1}H}-NCH_3 resonances all exhibit ^4J(PH) and

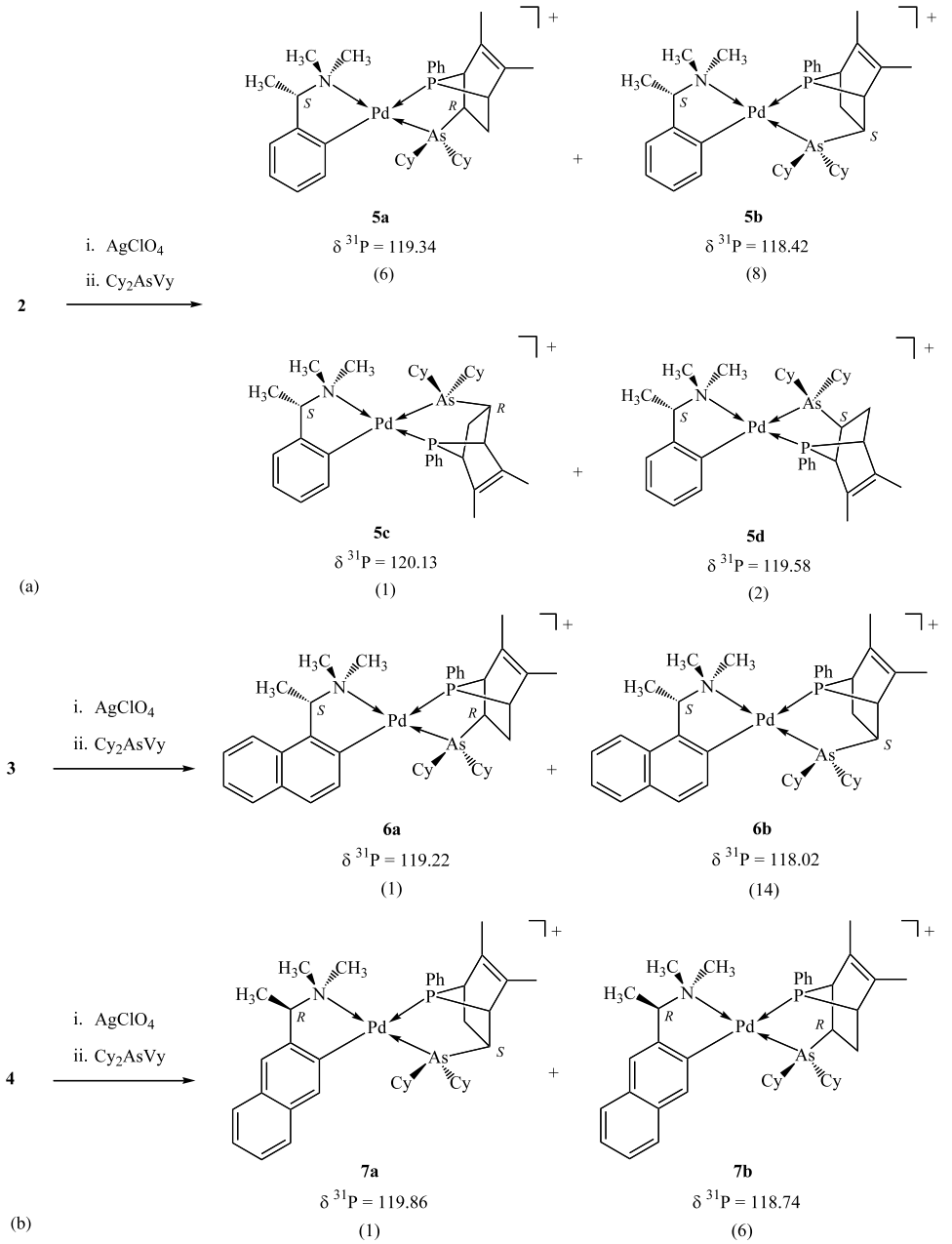

Scheme 2.

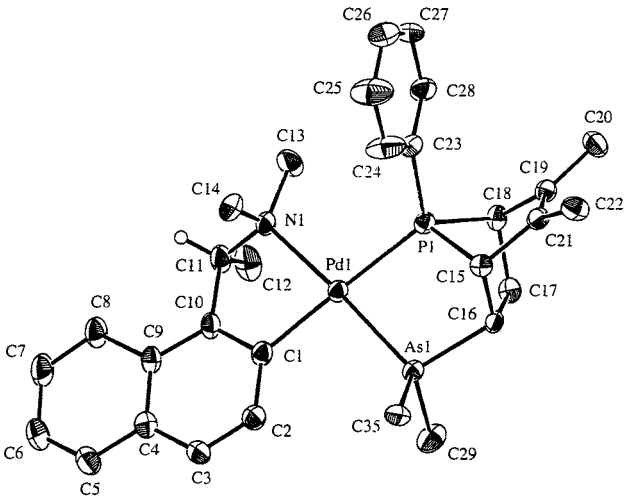

Fig. 4. Structural drawing of the cation of **6b** showing the atom numbering scheme (30% probability ellipsoids). The cyclohexyl ring carbon atoms have been removed for clarity. The hydrogen atom on C(11) has an arbitrary radius. Selected bond lengths (Å): Pd(1)–As(1), 2.3584(5); Pd(1)–P(1), 2.339(1); Pd(1)–N(1), 2.145(4); Pd(1)–C(1), 2.055(4); C(12)–C(21), 1.333(6) and angles (°): P(1)–Pd(1)–As(1), 82.39(3); As(1)–Pd(1)–C(1), 95.3(1); N(1)–Pd(1)–C(1), 80.8(2); P(1)–Pd(1)–N(1), 101.6(1).

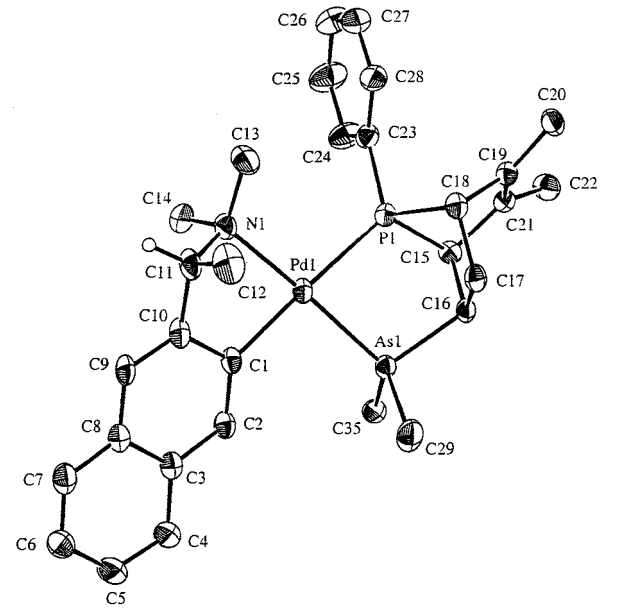

Fig. 5. Structural drawing of the cation of **7b** showing the atom numbering scheme (30% probability ellipsoids). The cyclohexyl ring carbon atoms have been removed for clarity. The hydrogen atom on C(11) has an arbitrary radius. Selected bond lengths (Å): Pd(1)–As(1), 2.3553(5); Pd(1)–P(1), 2.325(1); Pd(1)–N(1), 2.147(3); Pd(1)–C(1), 2.062(4); C(19)–C(21), 1.349(5) and angles (°): P(1)–Pd(1)–As(1), 82.70(3); As(1)–Pd(1)–C(1), 94.5(1); N(1)–Pd(1)–C(1), 80.9(1); P(1)–Pd(1)–N(1), 101.0(1).

^3J(PC) couplings of 2–5 Hz. The CH nuclei of the stereogenic carbon moiety are similarly coupled to phosphorus. The NMR data indicate that the phosphole is *trans* to nitrogen in all three complexes.

The crystal structure of **4** has previously been reported [17] and that of **3** is shown in Fig. 3. Selected bond distances and angles are given in Table 2. In both complexes the phosphole is *trans* to nitrogen, consistent with the NMR data. The palladium coordination geometry deviates slightly from planarity, having a small tetrahedral distortion. This is reflected in the non-zero dihedral angle between the P(1)–Pd(1)–Cl(1) and C(2)–Pd(1)–N(1) planes in **3** of 7.0(1)°. For both structures, the five-membered chelate ring is puckered. The Pd–C and Pd–N distances in **3** are slightly shorter than in **4** and the Pd–Cl and Pd–P distances are shorter in **4** than in **3**, but overall the two structures are similar.

Complexes **2**–**4** react with $AgClO_4$ and Cy_2AsVy (**1**) to give Diels–Alder [4 + 2] cycloaddition products in good chemical yields. As illustrated in Scheme 2, the reaction of **2** produces four diastereomeric Diels–Alder cycloadducts, whereas the reactions of **3** and **4** each produce two diastereomers. The major diastereomer formed from **3**, **6b**, and that formed from **4**, **7b**, were separated from the minor diastereomers and were fully characterized. The crystal structures of **6b** and **7b** are shown in Figs. 4 and 5, respectively. Clearly, the conversions of **3** into **6b** and **4** into **7b** involve ligand substitutions because arsenic is *trans* to nitrogen in **6b** and **7b**, whereas phosphorus is *trans* to nitrogen in **3** and **4**. It is likely that the ligand substitution precedes the cycloaddition for the following reasons. Diels–Alder cycloadditions of DMPP seldom occur with the free ligand [13,15] and when they do, there is no diastereoselectivity in contrast to that observed in the reactions described here. Moreover, several pairs of racemic diastereomers would be expected, (*syn–endo*, *syn–exo*, *anti–endo* and *anti–exo*) not the single *syn–exo* diastereomer that is produced by intramolecular cycloaddition within the coordination sphere of the chiral palladium template [15–17].

The $^{31}P\{^1H\}$-NMR chemical shift for **6b** (δ 118.02 ppm) is almost identical to that reported [16b] for the diphenylarsino analog **6c** (δ 118.1 ppm). Because the ^{31}P-NMR chemical shifts of **2** to **4** are so similar, we assign the structure of the major diastereomer formed from **2**, **5b**, to be the (S_CS_C) diastereomer (δ ^{31}P = 118.42 ppm) shown in Scheme 2. The minor diastereomer formed from **3**, **6a**, (δ ^{31}P = 119.22 ppm) is the(S_CR_C) diastereomer. By extension, the other diastereomers formed from **2** are the (S_CS_C), **5d**, and (S_CR_C), **5c**, diastereomers having phosphorus *trans* to nitrogen, as shown in Scheme 2. Compounds **7b** and **7a** are the (R_CR_C) and (R_CS_C) diastereomers (Scheme 2).

The ratio of diastereomers formed from **3** (14:1) and **4** (6:1) correspond to 87 and 71% diastereomeric excesses (d.e. values), respectively (%de = %major − %minor). The diastereoselectivity in the reaction of **2** is much lower (8:6:2:1). Consistent with the X-ray structures of **6b** and **7b**, neither the benzylic CH proton nor

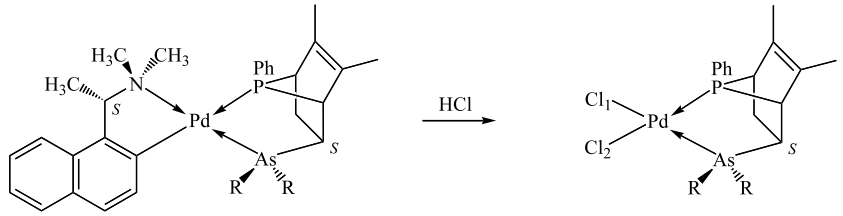

6 c R = Ph, δ ^{31}P = 118.1

6 b R = Cy, δ ^{31}P = 118.02

8 c R = Ph, δ ^{31}P = 129.4

8 b R = Cy, δ ^{31}P = 130.87

Scheme 3.

both of the NCH_3 carbon nuclei are coupled to phosphorus as is usually observed when phosphorus is *trans* to nitrogen in complexes of this type.

The amine can be removed from **6b**,**c** by protonation with HCl (Scheme 3). The crystal structures of **8c** [16b] and **8b** (Fig. 6) have been determined. Selected distances and angles in the two compounds are listed in Table 3. The absolute configurations of the stereocenters in both ligands are the same: R at P, C(1) and C(4) and *S* at C(2). Both complexes are distorted slightly from planarity with the angles at palladium ranging from 83.1(1) to 95.07(3). The smallest angle in both cases is the ligand bite angle, which differs little between the two compounds (83.61(2), **8b**; 83.1(1), **8c**). The Pd–P and Pd–As bond lengths are also very similar in the two structures and are unexceptional. In both structures, the Pd–Cl bond *trans* to phosphorus is slightly longer than that *trans* to arsenic, reflecting the greater *trans* influence of the phosphorus donor atom.

The proton and carbon chemical shifts of **8b** have been fully assigned and are given in the experimental section. COSY, APT, $^{1}H\{^{31}P\}$ and HETCOR (Fig. 7) spectra were used to make these assignments. From these spectra it was concluded that the cyclohexyl rings in the complex are locked in chair conformations with the arsenic atom in an equatorial position as found in the solid state structure. The $^{31}P\{^{1}H\}$ chemical shifts of **8c** (δ 129.4 ppm) and **8b** (δ 130.87 ppm) are very similar, indicating that the arsenic substituents have only a small effect on the ^{31}P chemical shift for ligands of this type (however, see Ref. [15k]).

Treatment of a dichloromethane solution of **8b** with aqueous sodium cyanide liberates the enantiomerically pure, very air-sensitive, arsinophosphine. Because of the extreme ease of oxidation of the free ligand it has not been isolated and characterized. This ligand reacts with $[(\eta^6\text{-arene})RuCl_2]_2$ (arene = $H_3CC_6H_5$, *p*-$H_3CC_6H_4$-CH_3), in the presence of NH_4PF_6, to form diastereomeric $[(\eta^6\text{-arene})Ru(P–As)Cl]PF_6$ complexes in which the ruthenium atom is a chiral stereocenter (Scheme 4). The diastereoselectivity of these reactions is rather low (**9a**:**9b** = 1:1.67, and **10a**:**10b** = 1:2.4). Diastereomer **9b** was separated from **9a** by fractional crystallization from CH_2Cl_2–*n*-hexane mixtures and fully characterized. The crystal structure of **9b** is shown in Fig. 8. The major diastereomer has the ($S_{Ru}S_C$) absolute configura-

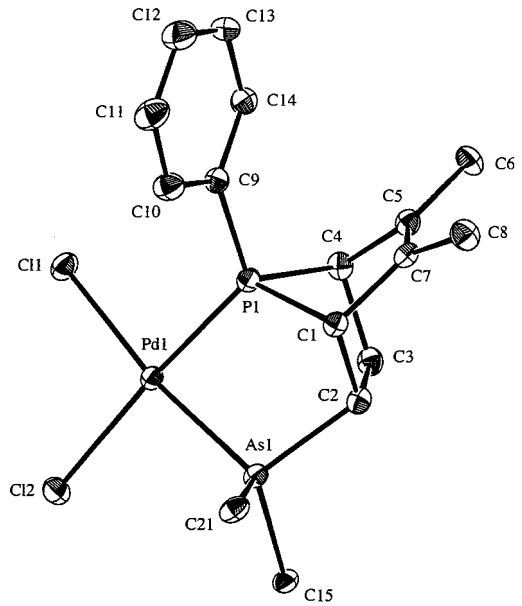

Fig. 6. Structural drawing of **8b** showing the atom numbering scheme (30% probability ellipsoids). The cyclohexyl ring carbon atoms have been removed for clarity.

Table 3
Selected bond distances (Å) and angles (°) **8c** and **8b**

Compound	**8c** [a]	**8b**
Bond distances		
Pd(1)–Cl1)	2.345(2)	2.3564(8)
Pd(1)–C1(2)	2.360(2)	2.3702(9)
Pd(1)–As(1)	2.349(1)	2.3584(9)
Pd(1)–P(1)	2.218(2)	2.2228(9)
Bond angles		
Cl(1)–Pd(1)–Cl(2)	94.78(9)	95.07(3)
Cl(1)–Pd(1)–P(1)	89.1(1)	88.72(3)
P(1)–Pd(1)–As(1)	83.1(1)	83.61(2)
As(1)–Pd(1)–Cl(2)	93.6(1)	92.53(2)

[a] Ref. [16b].

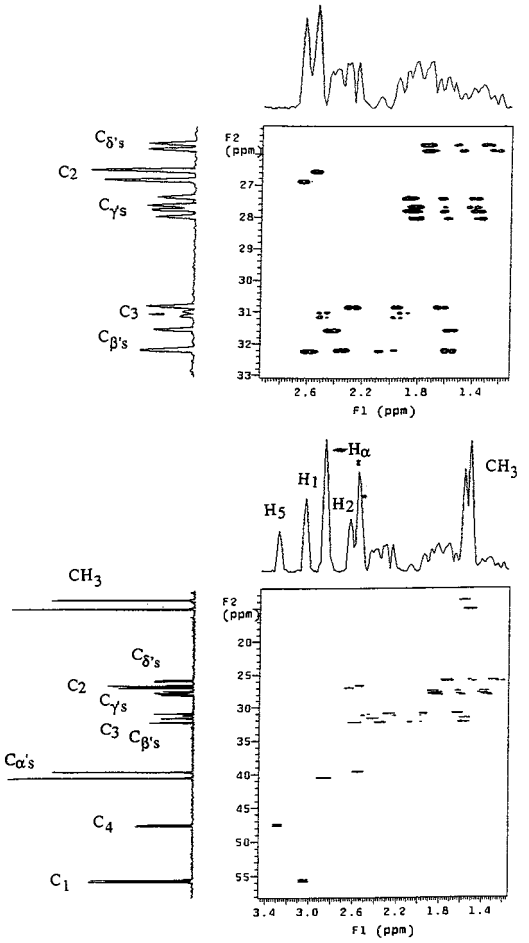

Fig. 7. Expansions of the 125 MHz HETCOR spectrum of **8b**. (a) Aliphatic region; (b) further expansion of the aliphatic region.

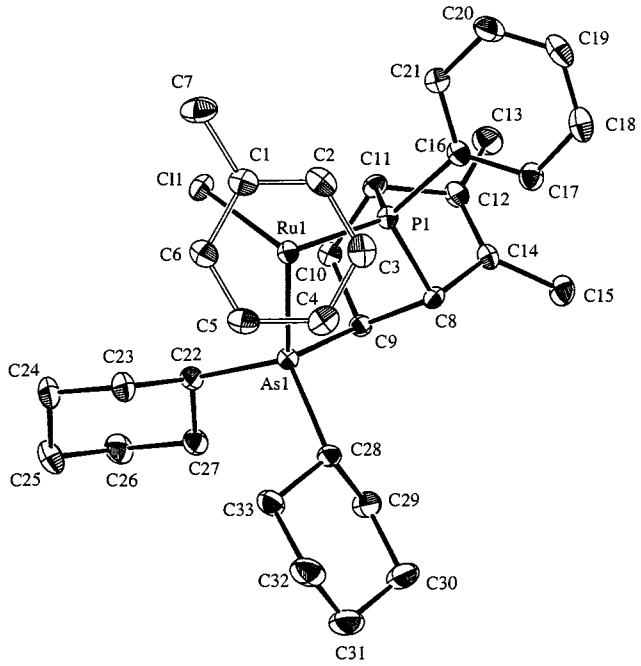

Fig. 8. Structural drawing of the cation of **9b** showing the atom numbering scheme (30% probability ellipsoids). Selected bond lengths (Å): Ru(1)–As(1), 2.4486(4); Ru(1)–Cl(1), 2.4074(9); Ru(1)–P(1), 2.2902(9); Ru–arene (average), 2.244(4) and angles (°): As(1)–Ru(1)–Cl(1), 88.73(2); As(1)–Ru(1)–P(1), 79.79; Cl(1)–Ru(1)–P(1), 90.30(3).

tion, which is usually found for complexes of this type [16k]. It crystallizes as discrete cations and anions with no unusual interionic contacts.

Diastereomers **10a** and **10b** could not be isolated in pure form, although the by-product **11** was separated

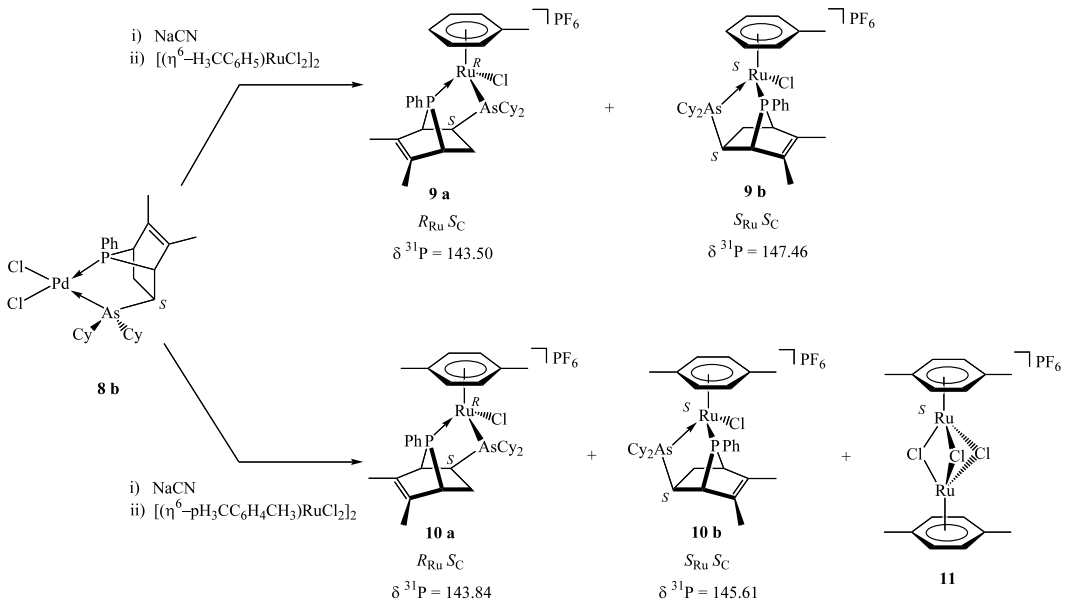

Scheme 4.

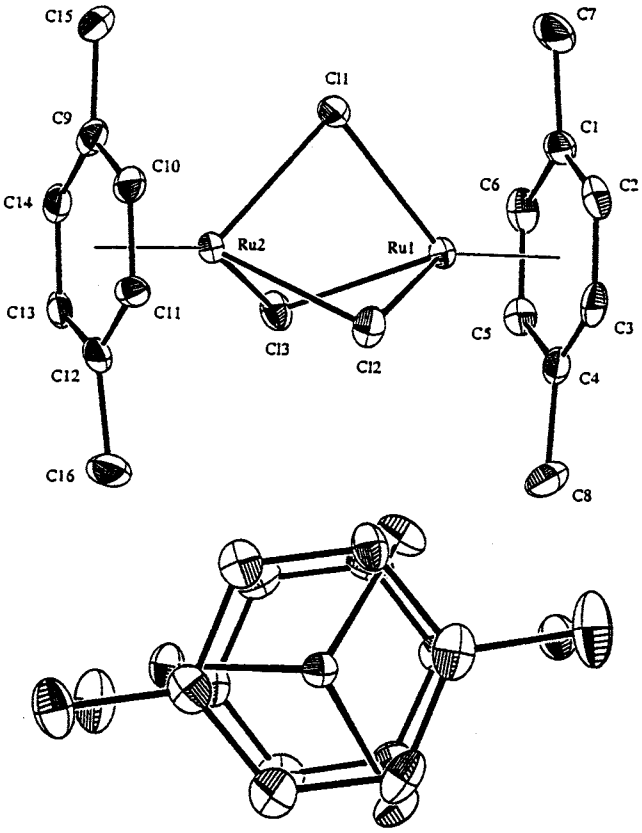

Fig. 9. Two views of the cation of **11** showing the atom numbering scheme (30% probability ellipsoids).

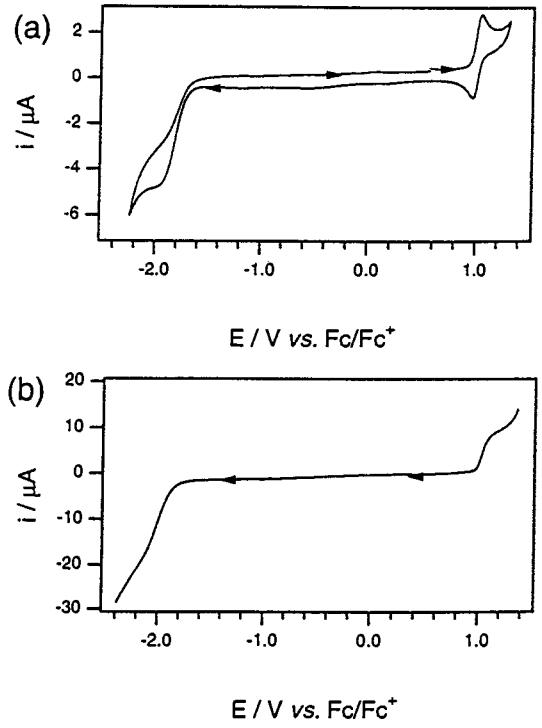

Fig. 10. Cyclic and rotating disc voltammograms of **9b** in CH_2Cl_2 at -50 °C.

from them by fractional crystallization and characterized. The crystal structure of **11** is shown in Fig. 9 and its metrical parameters are compared with those of analogous species in Table 4. The compound crystallizes as discrete cations and anions with no unusual interionic contacts. The cation has near D_{2h} symmetry with the two η^6-*p*-$H_3CC_6H_4CH_3$ planes parallel (dihedral angle 2.67) and eclipsed as was observed for the C_6H_6 [33,34] and $C_6(CH_3)_6$ [36] analogs. As is clear from the data presented in Table 4, the structure of the Ru_2Cl_3 core is almost identical in all of these complexes and there are only minor differences in the average Ru–C distances among the series of complexes.

There is considerable current interest in the configurational stability of chiral ruthenium(II) complexes [23] which bears directly on their application as asymmetric homogeneous catalysts. Ruthenium(III) species are believed to be involved as intermediates in catalytic C–H bond activation processes [37]. For these reasons we have studied, in some detail, the spectroelectrochemical behavior of enantiomerically pure **9b**. Similar to racemic analogs, **9b** undergoes a chemically reversible one-electron oxidation [$E_{1/2}$(II)/(III) = 1.02 V, $\Delta E = E_{Pc} - E_{Pa} = 60$ mV versus the ferrocene–ferrocenium couple] and a chemically irreversible two-electron reduction [E_{Pc}(II)/(0) = -1.98 V]. As can be seen in Fig. 10, the peak currents for these two electrochemical events have a two-to-one ratio consistent with their assignment as two- and one-electron processes, respectively. The stability of $\mathbf{9b}^+$ over time was confirmed by bulk electrolysis experiments (at -40 °C) which al-

Table 4
Structural data for [{(η^6-arene)Ru}$_2$μ-(Cl)$_3$]X complexes

Arene	X	Ru–Ru (Å)	Ru–Cl (average Å)	Ru–C (average Å)	Cl–Ru–Cl (average °)	Ru–Cl–Ru (average °)	Reference
C_6H_6	AsF_6	3.2754(4)	2.423	2.160	79.33	85.04	[33]
C_6H_6	BF_4	3.285(1)	2.432	2.163	NR [a]	84.99	[34]
$H_3CC_6H_5$	BF_4	3.275(1)	2.432	2.168	NR	84.66	[34]
p-$H_3CC_6H_4CH_3$	PF_6	3.2798(6)	2.440	2.167	79.75	84.49	This work
p-$H_3CC_6H_4CH(CH_3)_2$	BPh_4	3.282(3)	2.443	2.154	79.47	84.85	[35]
$C_6(CH_3)_6$	PF_6	3.278(3)	2.442	2.178	79.77	84.32	[36]

[a] NR, not reported.

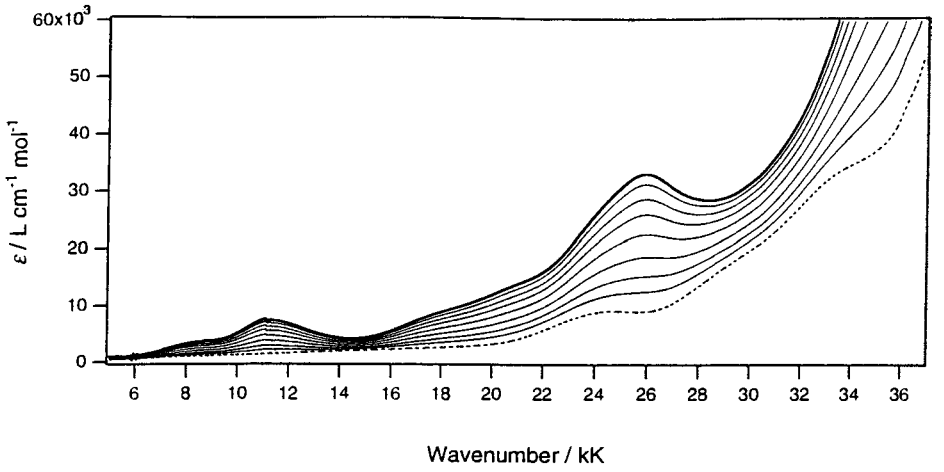

Fig. 11. Electronic spectra recorded during the one-electron oxidation of **9b** in CH_2Cl_2 at -50 °C. (---) First scan = **9b**. (=) Final scan = **9b**$^+$.

lowed the starting material to be quantitatively regenerated from the oxidized species over a period of several hours. Nevertheless, in order to ensure that **9b**$^+$ remained stable, the temperature needed to be maintained at ≤ -40 °C. Electrochemical and spectroscopic experiments showed that **9b**$^+$ decomposed within 2–3 min of warming to room temperature. Cyclic voltammetry experiments (Fig. 10) indicated that the two-electron reduced species was chemically unstable even over short voltammetric timescales (since no reverse oxidative peak was evident during cyclic voltammetry experiments), hence was unlikely to survive for enough time to allow spectroscopic characterization. The chemical reversibility of the Ru(II)/(III) process was confirmed by optical spectroelectrochemical measurements on chilled solutions of **9b** in CH_2Cl_2. The spectrum of theruthenium(II) complex, **9b**, exhibits absorptions similar in energy and intensity to those that we have reported for other three-legged piano stool rutheniu-m(II) complexes [38]. Upon progressive oxidation of **9b** to **9b**$^+$ in CH_2Cl_2 at -55 °C, and a constant applied potential of 1.2 V, a series of new bands appear and grow to their limiting intensities (Fig. 11). These new absorptions occur at 8.1 k Kaysers (kK) ($\varepsilon = 3 \times 10^{-3}$ l mol^{-1} cm^{-1}), 11.1 kK ($\varepsilon = 7 \times 10^3$ l mol^{-1} cm^{-1}), 18.1 kK ($\varepsilon = 7 \times 10^3$ lN mol^{-1} cm^{-1}), 20.6 kK ($\varepsilon = 1.3 \times 10^4$ l mol^{-1} cm^{-1}) and 25.9 kK ($\varepsilon = 3.3 \times 10^4$ l mol^{-1} cm^{-1}). Oxidation creates a low-lying hole on the metal center. A d-orbital splitting diagram, based upon descent in symmetry from an octahedral parentage, is shown in Fig. 12. As illustrated in this diagram, eight fully allowed d–d transitions could arise for this complex cation. However, the formally $d_{xy} \rightarrow d_{xz}$ and $d_{yz} \rightarrow d_{xz}$ transitions would be expected to occur near 3 kK and are thus too low in energy to appear in the region investigated. The new low-energy absorptions for this rather electropositive Ru(III) complex are in the region anticipated for ligand-to-metal charge transfer (LMCT) rich in As/P $\rightarrow$ Ru(III) character (8.1 and 11.1 kK). Both LMCT, especially Cl $\rightarrow$ Ru(III) and d–d excitations are anticipated to occur in the visible/near UV region (viz. 18.1, 20.6 and 25.9 kK) (see Fig. 12), with extensive mixing and/or intensity stealing in this low symmetry complex. The most intense band (36.5 kK) is probably dominated by a ligand based π/π^*

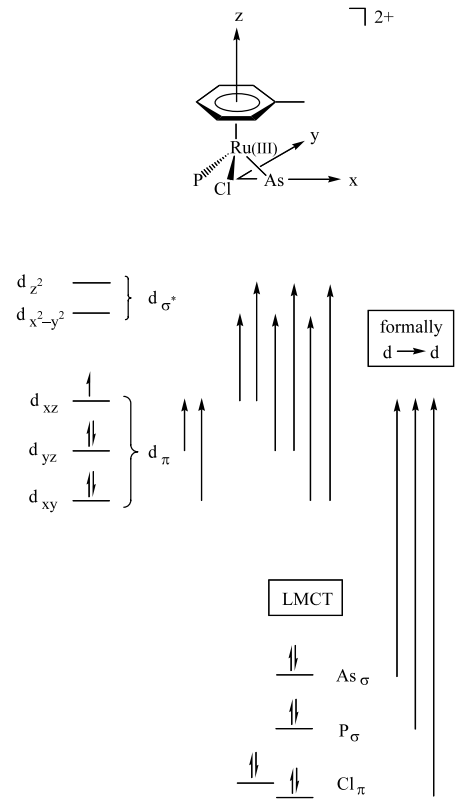

Fig. 12. Splitting diagram (d-orbital) for **9b** based upon descent in symmetry from an octahedral parent. The eight possible d–d electronic transitions are indicated by arrows on the diagram.

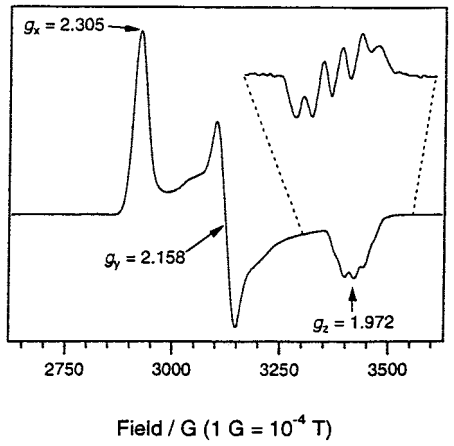

Fig. 13. First derivative EPR spectrum obtained on a 1.2 mM CH_2Cl_2 solution of **9b** at 5 K that had been exhaustively oxidized at 1.2 V. The inset shows an expanded second derivative in the g_z region. Modulation amplitude = 2G, microwave power = 0.2 mW.

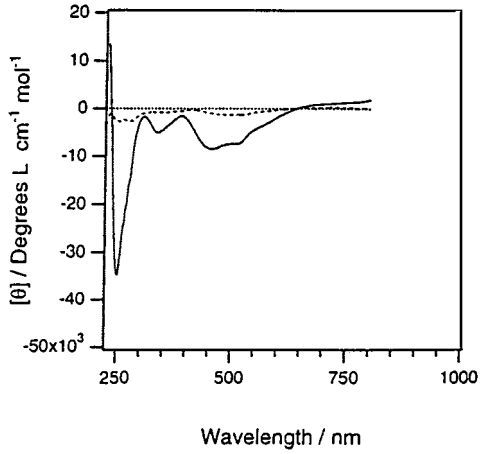

Fig. 14. Circular dichroism spectrum of **9b** in CH_2Cl_2 (solid line), baseline (dotted line), and difference spectrum (dashed line).

transition since a similar band is present in the spectra of divalent **9b** and the corresponding palladium complex, **8b**.

In order to better establish that a low-spin ruthenium(III) cation is indeed the product of one-electron oxidation of **9b**, the compound was exhaustively oxidized at 1.2 V and the EPR spectrum shown in Fig. 13 was obtained. The EPR spectrum (rhombic) may be interpreted [39] to indicate that the unpaired electron is principally localized on ruthenium in an unsymmetrical environment. This interpretation is supported by the observation of three g values, and the observation of hyperfine coupling to ^{99}Ru (I = 5/2, 12.72% natural abundance and ^{101}Ru (I = 5/2, 17.07%) natural abundance on g_y of 30 gauss. The observation of equivalent superhyperfine coupling to ^{75}As (I = 3/2) and ^{31}P (I = 1/2), both 100% natural abundance, on g_z of 25 gauss shows that the Ru–P and Ru–As bonds remain intact on the EPR time scale and confirms the importance of spin delocalization onto the ligands in this tervalent $4d^5$ cation. Few EPR spectra of ruthenium(III) complexes exhibit this much detail [39].

The configurational stability of the ruthenium stereocenter in **9b** during redox cycling was probed by circular dichroism spectroscopy. Figs. 14 and 15 show the circular dichroism spectra of **9b** and of $\mathbf{9b}^+$ formed by exhaustive oxidation at 1.2 V. Comparison of Figs. 11 and 15 affirms the location of transitions observed only as shoulders in the electronic spectrum (Fig. 11), and reveals long-wavelength features that are too weak to be resolved in the optical spectra of d^6 **9b**. Several of the transitions in Fig. 15 are metal centered and demonstrate that the Ru(III) ion in $\mathbf{9b}^+$ still has a single absolute configuration. Epimerization does not occur upon oxidation at low temperature. A difference spectrum is also shown in Fig. 14. This trace represents the difference between the spectrum of pristine **9b** and a solution of **9b** after exhaustive electrolytic oxidation and reduction, all at low temperature. The spectrum

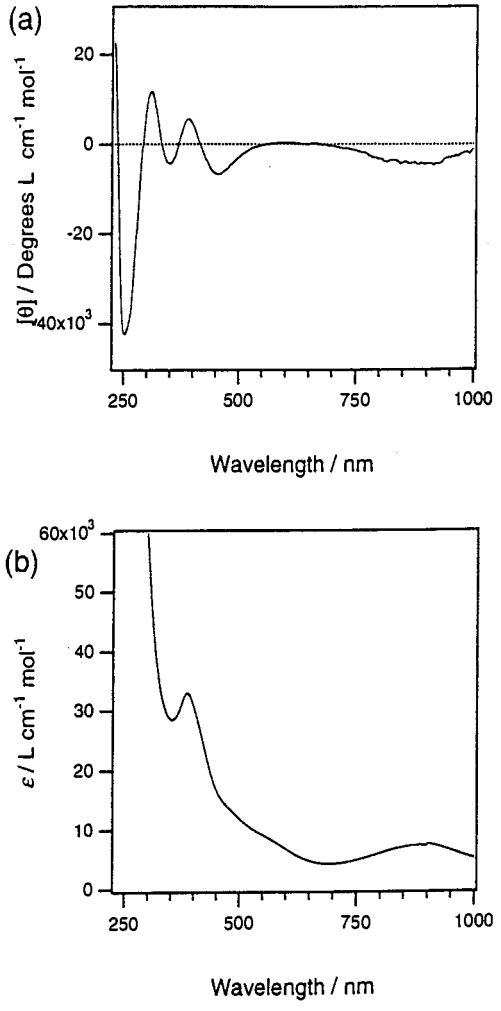

Fig. 15. (a) Circular dichroism spectrum of **9b** plus $NBu^n_4PF_6$ in CH_2Cl_2 (−40 °C) after exhaustive oxidation at 1.2 V. $[\theta]_{914} = -5000$, $[\theta]_{620} = 0$, $[\theta]_{455} = -8000$, $[\theta]_{408} = 0$, $[\theta]_{390} = +5000$, $[\theta]_{378} = 0$, $[\theta]_{350} = -5000$, $[\theta]_{329} = 0$, $[\theta]_{318} = +12{,}000$, $[\theta]_{280} = 0$, $[\theta]_{251} = -42000$, $[\theta]_{230} = 0$. (b) UV–vis–NIR spectrum.

was recorded 24 h later on the resulting Ru(II) solution at ambient temperature. This spectrum demonstrates that at least 99% of **9b** has retained its absolute configuration during the redox process. From these data we conclude that both **9b** and **9b**$^+$ are configurationally stable at low temperature. At room temperature the ruthenium(II) complex is indefinitely inert to epimerization but the oxidized complex, **9b**$^+$, decomposes to unidentified species at temperatures above -20 °C.

4. Conclusions

The chiral palladium templates in **2**–**4** provide fair to good asymmetric induction for intramolecular [4 + 2] Diels–Alder cycloadditions between 3,4-dimethyl-1-phenylphosphole and the sterically bulky dieneophile dicyclohexylvinylarsine. In each case, ligand substitution of the phosphole by the arsine preceded the cycloaddition reaction. The diastereoselectivity of the reactions is strongly related to the structure of the cyclopalladated amine, with the order of the diastereoselectivity being **3** > **4** > **2**. These observations most likely have a subtle steric origin that derives from the relative magnitudes of interactions among the ligands within the palladium coordination sphere in each case. Complex **2** has been previously shown, [40] to undergo a diastereoselective Diels–Alder cycloaddition with $Ph_2PCH{=}CH_2$ but gave poor results with a few other dieneophiles. The new conformationally rigid, sterically encumbered, chiral arsinophosphine can be liberated from palladium and transferred to ruthenium. The chiral ruthenium(II) complexes that result were formed with low diastereoselectivities. Spectroscopic measurements have established that electrogenerated **9b**$^+$ is a well-defined and long-lived species in its own right despite its highly oxidizing nature and that there is no measurable epimerization in the course of the bulk Ru(II)/Ru(III)/Ru(II) redox transformation. The derived Ru(III) complex, **9b**$^+$, decomposes at temperatures above about -20 °C.

5. Supplementary material

Tables of X-ray data in CIF format for compounds **3**, **6b**, **7b**, **8b**, **9b** and **11** have been deposited with the Cambridge Crystallographic Data Centre, nos. 164051–164055 and 164865. Copies of this information may be obtained free of charge from The Director, CCDC, 12 Union Road, Cambridge CB2 1EZ, UK (Fax: +44-1223-336033; e-mail: deposit@ccdc.cam.ac.uk or www: http://www.ccdc.cam.ac.uk).

References

[1] F. Mathey, J. Fischer, J.H. Nelson, Struct. Bonding (Berlin) 55 (1983) 153.
[2] F. Mathey, Angew. Chem. Int. Ed. Engl. 26 (1987) 275.
[3] F. Mathey, Chem. Rev. 88 (1988) 429.
[4] L.M. Wilkes, J.H. Nelson, L.B. McCusker, K. Seff, F. Mathey, Inorg. Chem. 22 (1983) 2476.
[5] M.S. Holt, J.J. MacDougall, F. Mathey, J.H. Nelson, Inorg. Chem. 23 (1984) 449.
[6] F. Mercier, F. Mathey, J. Fischer, J.H. Nelson, J. Am. Chem. Soc. 106 (1984) 425.
[7] F. Mercier, F. Mathey, J. Fischer, J.H. Nelson, Inorg. Chem. 24 (1985) 4141.
[8] J.H. Nelson, F. Mathey, in: J.G. Verkade, L.D. Quin (Eds.), ^{31}P-NMR Spectroscopy, Verlag Chemie, Deerfield Beach, FL, 1987, pp. 665–694.
[9] K.D. Dillon, F. Mathey, J.F. Nixon (Eds.), Phosphorus—The Carbon Copy, Wiley, Chichester, 1998.
[10] N.S. Isaacs, G.N. El-Din, Tetrahedron 45 (1989) 7083.
[11] G. Kegevich, M. Treska, B. Dajka, B. Peta, A. Dobo, L. Toke, Heteroatom Chem. 11 (2000) 271.
[12] F. Mathey, F. Mercier, Tetrahedron Lett. 22 (1981) 319.
[13] E. Mattmann, D. Simonutti, L. Ricard, F. Mercier, F. Mathey, J. Org. Chem. 66 (2001) 755.
[14] P.V.R. Schleyer, P.K. Freeman, H. Jiao, B. Goldfuss, Angew. Chem. Int. Ed. Engl. 34 (1995) 337.
[15] (a) M.S. Holt, J.H. Nelson, P. Savignac, N.W. Alcock, J. Am. Chem. Soc. 107 (1985) 6396;
(b) R.L. Green, J.H. Nelson, J. Fischer, Organometallics 6 (1987) 2556;
(c) J.A. Rahn, M.S. Holt, G.A. Gray, N.W. Alcock, J.H. Nelson, Inorg. Chem. 28 (1989) 217;
(d) Lj. Solujić, E.B. Milosavljević, J.H. Nelson, N.W. Alcock, J. Fischer, Inorg. Chem. 28 (1989) 3453;
(e) S. Affandi, J.H. Nelson, J. Fischer, Inorg. Chem. 28 (1989) 4536;
(f) D. Bhaduri, J.H. Nelson, C.L. Day, R.A. Jacobson, Lj. Solujić, E.B. Milosavljević, Organometallics 11 (1992) 4069;
(g) H.-L. Ji, J.H. Nelson, A. De Cian, J. Fischer, Lj. Solujić, E.B. Milosavljević, Organometallics 11 (1992) 1840;
(h) J.H. Nelson, in: L.D. Quin, J.G. Verkade (Eds.), Phosphorus-31—NMR Spectral Properties in Compound Characterization and Structural Analysis, VCH, Deerfield Beach, FL, 1994, pp. 203–214;
(i) K. Maitra, V.J. Catalano, J.H. Nelson, J. Am. Chem. Soc. 119 (1997) 12560;
(j) K.D. Redwine, V.J. Catalano, J.H. Nelson, Syn. React. Inorg. Met. Org. Chem. 29 (1999) 395;
(k) K.D. Redwine, J.H. Nelson, J. Organomet. Chem. 613 (2000) 177.
[16] (a) P.-H. Leung, S.K. Loh, K.F. Mok, A.J.P. White, D.J. Williams, J. Chem. Soc. Chem. Commun. (1996) 591;
(b) B.H. Aw, P.-H. Leung, A.J.P. White, D.J. Williams, Organometallics 15 (1996) 3640;
(c) S. Selvaratnam, K.F. Mok, P.-H. Leung, A.J.P. White, D.J. Williams, Inorg. Chem. 35 (1996) 4798;
(d) P.-H. Leung, S.K. Loh, K.F. Mok, A.J.P. White, D.J. Williams, J. Chem. Soc. Dalton Trans. (1996) 4443;
(e) B.H. Aw, T.S.A. Hor, S. Selvaratnam, A.J.P. White, D.J. Williams, N.H. Rees, W. McFarlane, P.-H. Leung, Inorg. Chem. 36 (1997) 2138;
(f) P.-H. Leung, S. Selvaratnam, C.R. Cheng, K.F. Mok, N.H. Rees, W. McFarlane, J. Chem. Soc. Chem. Commun. (1997) 751;
(g) A.M. Liu, K.F. Mok, P.-H. Leung, J. Chem. Soc. Chem. Commun. (1997) 2397;

(h) P.-H. Leung, S.Y. Siah, A.J.P. White, D.H. Williams, J. Chem. Soc. Dalton Trans. (1998) 893;
(i) Y. Song, J.J. Vittal, S.-H. Chan, P.-H. Leung, Organometallics 18 (1999) 650;
(j) P.-H. Leung, G. He, H. Lang, A. Liu, S.K. Loh, S. Selvaratnam, K.F. Mok, A.J.P. White, D.J. Williams, Tetrahedron 56 (2000) 7;
(k) P.-H. Leung, Y. Qin, G. He, K.F. Mok, J.J. Vittal, J. Chem. Soc. Dalton Trans. (2001) 309.
[17] N. Gül, J.H. Nelson, Tetrahedron 56 (2000) 71.
[18] (a) E.J. Corey, H.E. Ensley, J. Am. Chem. Soc. 97 (1975) 6908;
(b) S.L. Hashimoto, N. Komeshima, K. Koga, J. Chem. Soc. Chem. Commun. (1979) 437;
(c) M. Petrzilka, J.I. Grayson, Synthesis (1981) 753;
(d) M. Bednarski, S. Danishefski, J. Am. Chem. Soc. 105 (1983) 3716;
(e) W. Oppolzer, in: B.M. Trost (Ed.), Comprehensive Organic Synthesis, vol. 5, Pergamon, Oxford, 1991 Chapter 4.
[19] (a) K. Mashima, K. Kusano, T. Ohta, R. Noyori, H. Takahya, J. Chem. Soc. Chem. Commun. (1989) 1208;
(b) K. Püntener, L. Schwink, P. Knochel, Tetrahedron Lett. 37 (1996) 8165.
[20] T. Ohta, T. Miyake, H. Takaya, J. Chem. Soc. Chem. Commun. (1992) 1725.
[21] N. Uematsu, A. Fujii, S. Hashiguchi, T. Ikariya, R. Noyori, J. Am. Chem. Soc. 36 (1996) 288.
[22] (a) U. Matteoli, P. Frediani, M. Bianchi, C. Botteghi, S. Gladiali, J. Mol. Catal. 12 (1981) 265;
(b) T.M. Trinka, R.H. Grubbs, Acc. Chem. Res. 34 (2001) 18.
[23] (a) H. Brunner, Adv. Organomet. Chem. 18 (1980) 151;
(b) G. Consiglio, F. Morandini, Chem. Rev. 87 (1987) 761;
(c) H. Brunner, Angew. Chem. Int. Ed. Engl. 38 (1999) 1194;
(d) G.C. Martin, J.M. Boncella, Organometallics 8 (1989) 2968;
(e) S.K. Mandal, A.R. Chakravarty, J. Organomet. Chem. 417 (1991) C59;
(f) S.K. Mandal, A.R. Chakravarty, J. Chem. Soc. Dalton Trans. (1992) 1627;
(g) S.K. Mandal, A.R. Chakravarty, Inorg. Chem. 32 (1993) 3851;
(h) W.J. Grigsby, L. Main, B.K. Nicholson, Organometallics 12 (1993) 397;
(i) F. Masarani, M. Pfeffer, I. Spencer, E. Wehman, J. Organomet. Chem. 220 (1994) 115;
(j) H. Brunner, R. Oeschey, B. Nuber, Angew. Chem. Int. Ed. Engl. 33 (1994) 866;
(k) S. Attar, J.H. Nelson, J. Fischer, A. De Cian, J.-P. Sutter, M. Pfeffer, Organometallics 14 (1995) 4559;
(l) H. Brunner, R. Oeschey, B. Nuber, Inorg. Chem. 34 (1995) 3349;
(m) S. Attar, V.J. Catalano, J.H. Nelson, Organometallics 15 (1996) 2932;
(n) H. Brunner, R. Oeschey, B. Nuber, J. Chem. Soc. Dalton Trans. (1996) 1499;
(o) H. Brunner, R. Oeschey, B. Nuber, Organometallics 15 (1996) 3616;
(p) H. Brunner, R. Oeschey, B. Nuber, J. Organomet. Chem. 518 (1996) 47;
(q) H.D. Hansen, K. Maitra, J.H. Nelson, Inorg. Chem. 38 (1999) 2150;
(r) N. Gül, J.H. Nelson, Organometallics 18 (1999) 709;
(s) N. Gül, J.H. Nelson, Polyhedron 18 (1999) 1835;
(t) H. Brunner, T. Zwack, Organometallics 19 (2000) 2423.
[24] A. Bregue, F. Mathey, P. Savignac, Synthesis (1981) 983.
[25] (a) D.G. Allen, G.M. McLaughlin, G.B. Robertson, W.L. Steffan, G. Salem, S.B. Wild, Inorg. Chem. 21 (1982) 1007;
(b) K. Tani, L.D. Grown, J. Ahmed, J.A. Ibers, M. Yokota, A. Nakamura, S. Otsuka, J. Am. Chem. Soc. 99 (1977) 7876.
[26] M.A. Bennett, A.K. Smith, J. Chem. Soc. Dalton Trans. (1974) 233.
[27] C.M. Duff, G.A. Heath, Inorg. Chem. 30 (1991) 2528; J. Chem. Soc. Dalton Trans. (1991) 2401.
[28] A. Tschach, W. Lange, Z. Anorg, Allg. Chem. 326 (1964) 280.
[29] P. Copens, in: F.R. Ahmed, S.R. Hall, C.P. Huber (Eds.), Crystallographic Computing, Munksgaard, Copenhagen, 1970, pp. 255–270.
[30] International Tables for X-ray Crystallography, vol. C, D. Reidell Publishing Co., Boston, 1992.
[31] H.D. Flack, Acta Crystallogr. Sect. A 39 (1983) 876.
[32] N. Gül, J.H. Nelson, Organometallics 19 (2000) 91.
[33] F.B. McCormic, W.B. Gleason, Acta Crystallogr. Sect. C 49 (1993) 1493.
[34] F. Grepioni, D. Braga, P.J. Dyson, B.F.G. Johnson, F.M. Sanderson, M.J. Calhorda, L.F. Veiros, Organometallics 14 (1995) 121.
[35] D.A. Tocher, M.D. Walkinshaw, Acta Crystallogr. Sect. B 38 (1982) 3083.
[36] K.D. Redwine, H.D. Hansen, S. Bowley, J. Isbell, M. Sanchez, D. Vodak, J.H. Nelson, Syn. React. Inorg. Met.-Org. Chem. 30 (2000) 379.
[37] A. Ceccanti, P. Diversi, G. Ingrosso, F. Laschi, A. Lucherini, S. Magagna, P. Zanello, J. Organomet. Chem. 526 (1996) 251.
[38] H.-L. Ji, J.H. Nelson, A. DeCian, J. Fischer, B. Li, C. Wang, B. McCarty, Y. Aoki, J.W. Kenny, Lj. Solujić III, E.B. Milosavljević, J. Organomet. Chem. 529 (1997) 395.
[39] P.H. Rieger, Coord. Chem. Rev. 135/136 (1994) 203.
[40] S. Selvaratnam, P. P.-H. Leung, A.J.P. White, D.J. Williams, J. Organomet. Chem. 542 (1997) 61.